Understanding the Influence of Alloy Chemistry on Heat Treatment Process Windows

Paul Mason

Thermo-Calc Software

Thermo-Calc Software

Chemical Composition

Properties
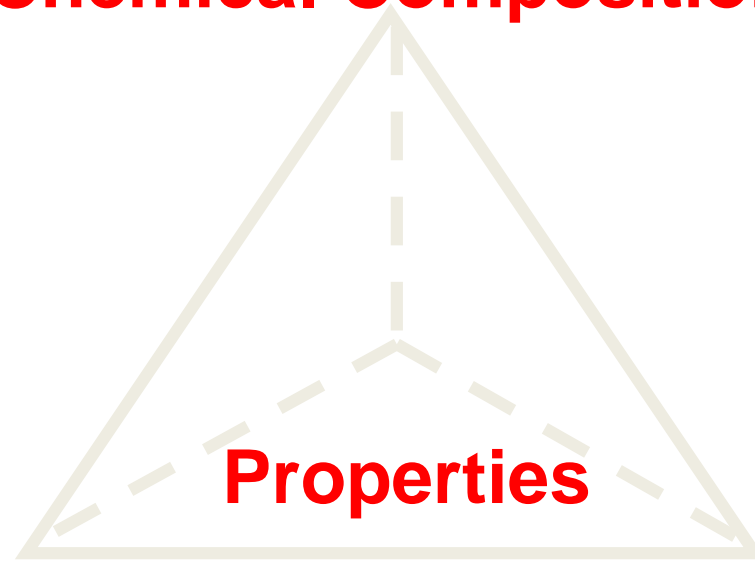
Microstructure   **Processing**

Heat treating can best be defined as "the <u>controlled application</u> of <u>time, temperature and atmosphere</u> to produce a <u>predictable</u> <u>change</u> in the internal structure (i.e. <u>the microstructure</u>) of a material." Dan Herring, 100th Column of the "Heat Treat Doctor" published in Industrial Heating magazine

Objectives

During this webinar, you will learn:

- What is the CALPHAD approach

- How CALPHAD can be applied to heat treatment processes:

  - How actual chemistries influence processing windows and transformation temperatures such as liquidus, solidus, A1, A3, Ms

  - The influence of alloy chemistry and temperature on diffusion and how this affects carburizing, nitriding, homogenization, etc.

  - How precipitation of secondary phases can be predicted as a function of chemistry, temperature and time.

  - Calculate furnace activities based on gas composition and temperature

  - How these types of calculations can be employed in production environments.

Outline

- Introduction to CALPHAD

- Application examples
  - Homogenization
  - Annealing / aging
  - Surface hardening
  - Stress relief (additive manufacturing)
  - Quenching (Martensite and pearlite)

- Questions

  Examples will cover a range of alloys including steels, Ni and Al alloys

Influence of processing on microstructure and properties

Properties depend on processing and resultant microstructure

AlSi10Mg alloy produced through gravity casting (a) and AM (b)
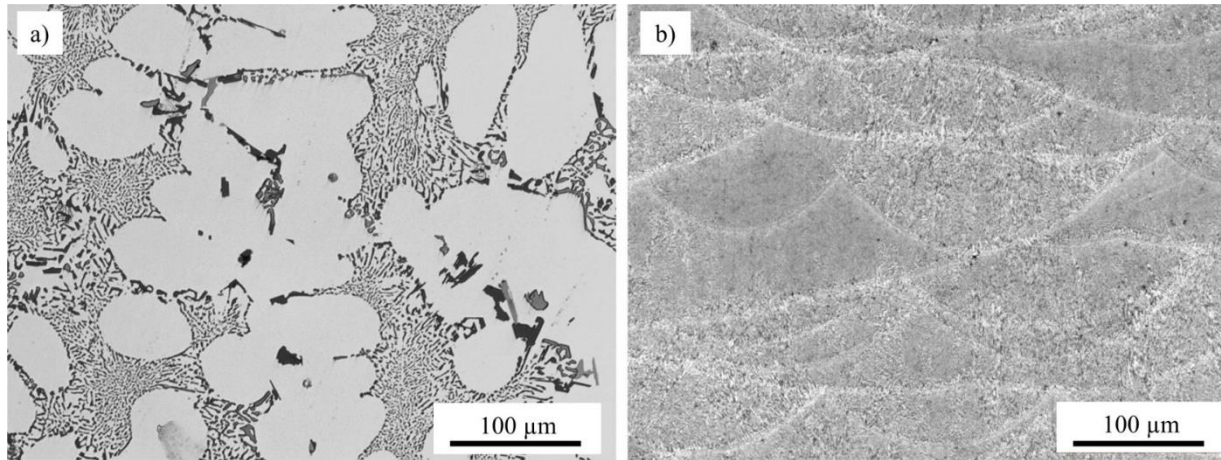
Fabio Boiocchi, Metalworking World Magazine (2019)

Composition — Processing — Structure — Properties — Performance
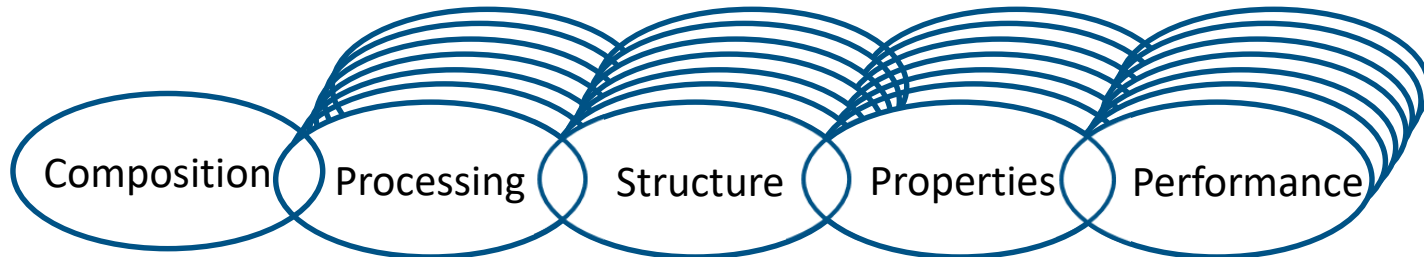
Influence of chemistry on microstructure and properties

CHEMICAL COMPOSITION

ELEMENT	WEIGHT %	
	Min.	Max.
Aluminum	5.50	6.50
Tin	1.80	2.20
Zirconium	3.60	4.40
Molybdenum	1.80	2.20
Silicon	0.06	0.13
Iron	—	0.25
Oxygen	—	0.15
Carbon	—	0.08
Nitrogen	—	0.05
Hydrogen	0.010	0.0125
Residual Elements, each	—	0.10
Residual Elements, total	—	0.40
Titanium	Remainder	
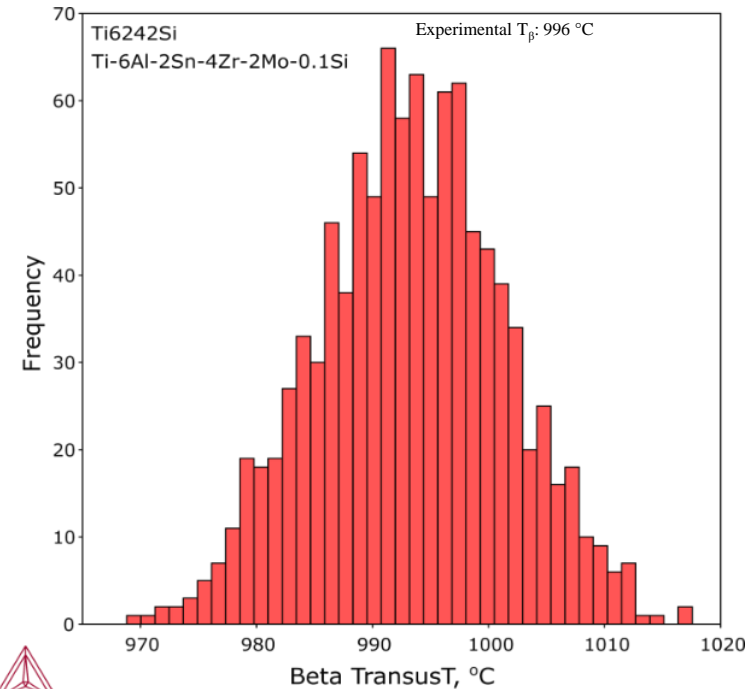
Composition variation within the material specification range
can result in different properties

Composition dependence: Almost infinite space

Thermo-Calc Software
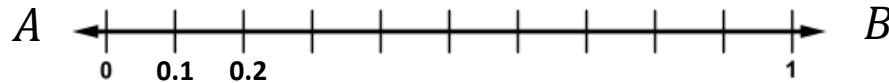
A — B Many potential combinations!

0   0.1   0.2   1

n = # elements = 2 (i.e. A and B)

k = # steps = 10 => **11 combinations** k = # steps = 100 => **101 combinations**

For an alloy with 10 elements:
n=10 and k=100 (i.e. steps of 1%) => $\mathbf{10^{12}}$

Taking all elements in our Ni-database:
n=30 and k=100 (i.e. steps of 1%) => $\mathbf{10^{27}}$

Our universe has existed for $< 10^{18}$ *seconds*

Unlimited design space!

…and only an infinitesimally small fraction of that possible composition space has been explored.

Traditional Sources of data
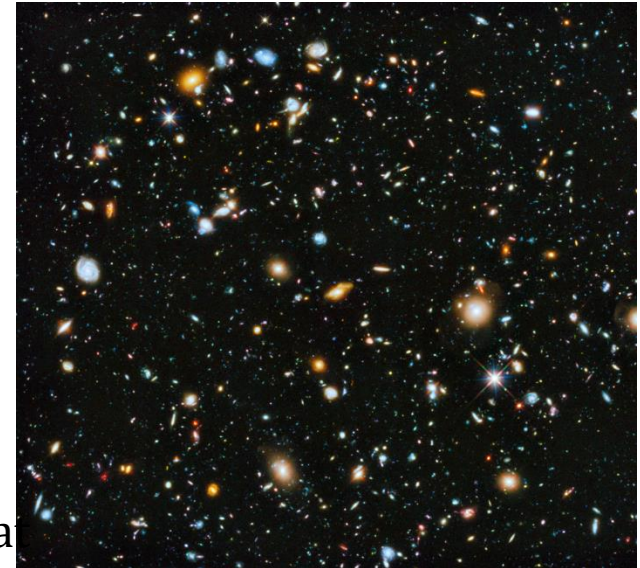
Experiments

- Costly
- Time Consuming
- Need more experiments for each new material or novel process.
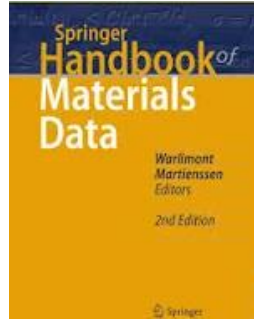
Handbooks

- A typical handbook contains data for < 1000 alloys
- And far from all properties of interest
- Data lacking for new alloy design / materials discovery
- Data not always applicable to new processes (e.g. additive)

Alternative: data can be simulated or estimated

- Mechanistic models
- Phenomenological models
- Machine Learning
- Ab Initio/Molecular dynamics
- Regression analysis

The needed knowledge structure

Goal/means
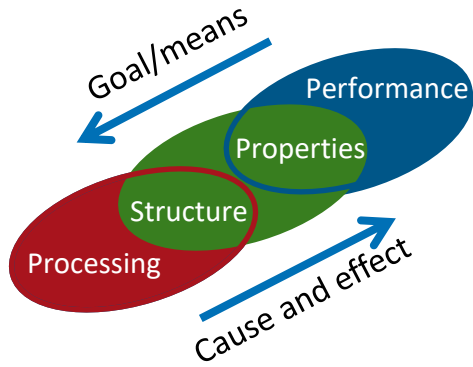
Performance

Properties

Structure

Processing

Cause and effect

Properties

C. Liebscher

The recipe:

Composition / Processing

Performance

SKF Aerospace
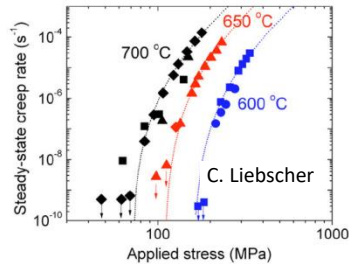
To describe these links we need _models_, but all models need _data_, so this is needed too.

Structure

A. Piglione

Thermo-Calc Software

CALculation of PHAse Diagrams

- ❑ A phase-based approach which captures the composition and temperature dependence of properties in a self consistent framework.

- ❑ Databases are developed through the fitting of binary and ternary systems and extrapolated to multicomponent systems.

- ❑ Applicable to "real" engineering materials.

- ❑ Extendable far beyond traditional thermochemistry.
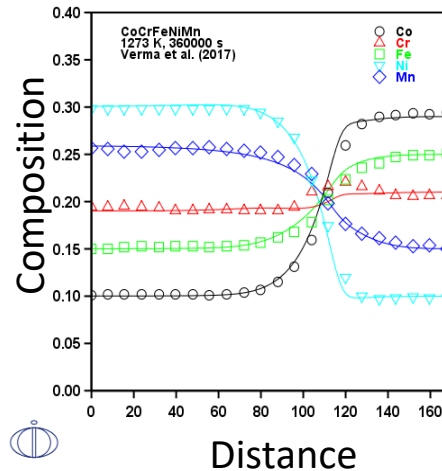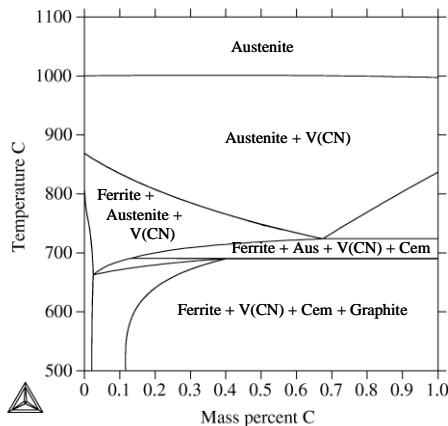
$$G(p,T) = H - TS$$

Gibbs Free Energy

$$\frac{\partial C}{\partial t} = D \frac{\partial^2 C}{\partial x^2}$$

Ficks Laws of Diffusion

$$\Delta G = \frac{4}{3}\pi r^3 \Delta g + 4\pi r^2 \sigma$$

Classical Nucleation Theory

Thermodynamic Databases (*The CALPHAD approach*)

Thermochemical measurements:

- Enthalpy
- Entropy
- Heat capacity
- Activity

Phase equilibria:

- Liquidus
- Solidus
- Phase boundary

Gibbs Energy of Individual Phases

$$G_m^\alpha = f(x, T, P)$$

Applications
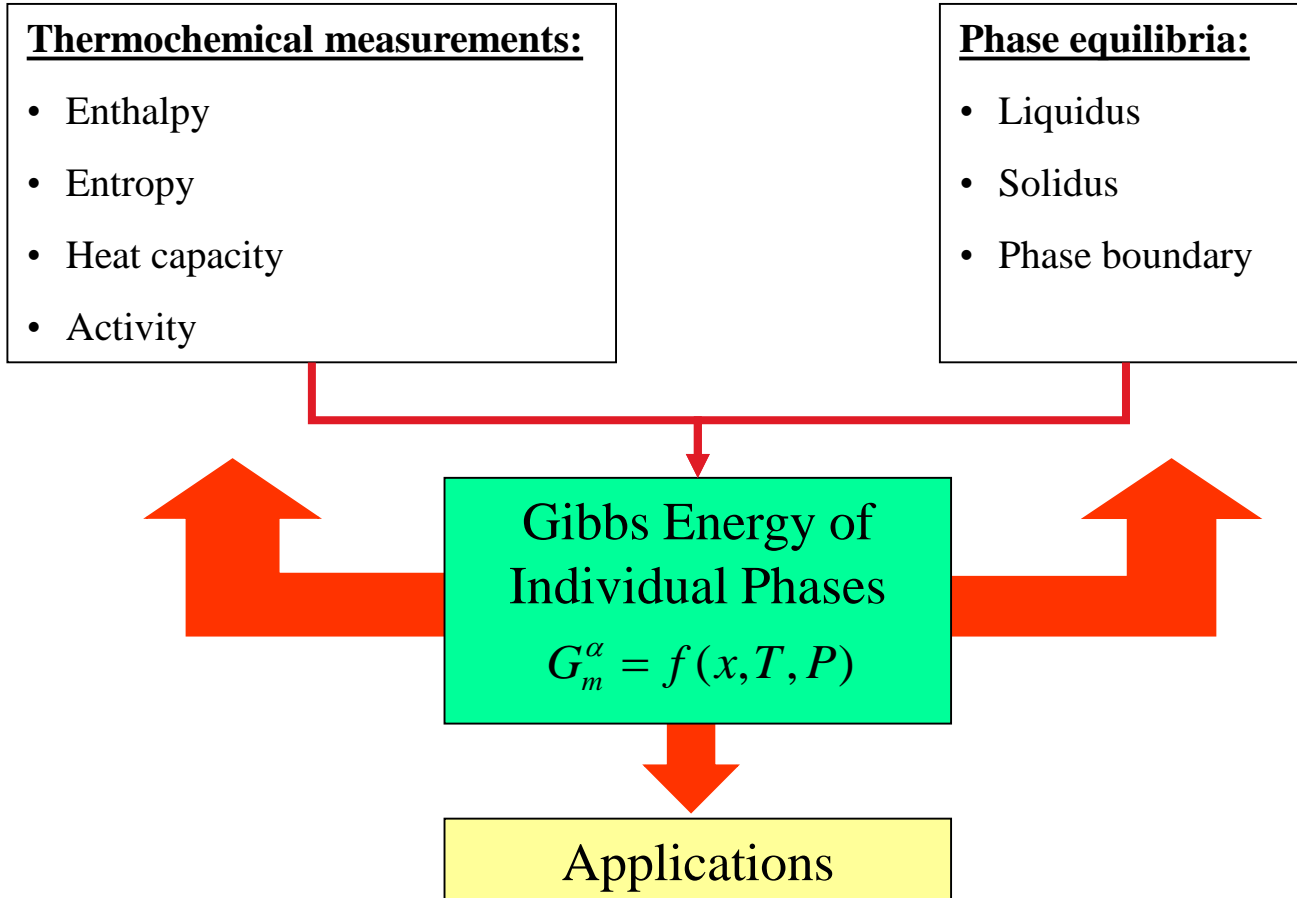
Databases based on binary and ternary systems

Thermo-Calc Software

TCNI8

Assessed binary systems

	Al	B	C	Co	Cr	Cu	Fe	Hf	Mn	Mo	N	Nb	Ni	O	Pd	Pt	Re	Ru	Si	Ta	Ti	V	W	Y
B	x																							
C	x	x																						
Co	x	x	x																					
Cr	x	x	x	x																				
Cu	x	x	x	x	x																			
Fe	x	x	x	x	x	x																		
Hf	x	x	x	x	x	x	x																	
Mn	x	x	x	x	x	x	x	x																
Mo	x	x	x	x	x	x	x																	
N	x	x		x	x	x	x		x	x														
Nb	x	x	x	x	x	x	x	x	x	x	x													
Ni	x	x	x	x	x	x	x	x	x	x	x	x												
O	x	x		x	x	x	x	x		x	x	x	x											
Pd	x	x	x	x	x	x	x	x	x	x		x	x	x										
Pt	x	x	x	x	x	x	x	x	x	x		x	x	x	x									
Re	x	x	x	x	x	x	x	x	x	x		x	x	x	x									
Ru	x	x	x	x	x	x	x	x	x	x		x	x	x	x									
Si	x	x	x	x	x	x	x	x	x	x	x	x	x	x	x	x	x	x						
Ta	x	x	x	x	x	x	x	x	x	x	x	x	x	x	x	x	x	x	x					
Ti	x	x	x	x	x	x	x	x	x	x	x	x	x	x	x	x	x	x	x	x				
V	x	x	x	x	x	x	x	x	x	x	x	x	x	x	x	x	x	x	x	x	x			
W	x	x	x	x	x	x	x	x	x	x	x	x	x	x	x	x	x	x	x	x	x	x		
Y	x	x	x	x	x	x	x	x	x	x	x	x	x	x	x	x	x	x	x	x	x	x	x	
Zr	x	x	x	x	x	x	x	x	x	x	x	x	x	x	x	x	x	x	x	x	x	x	x	x

280 assessed binary systems in full range of composition and temperature

Assessed ternary systems

Al-B-Co	Al-Cr-O	Al-Nb-Ni	B-Cr-Ni	C-Cr-W	C-Ti-W	Co-O-Si	Cr-Ni-Ti	Fe-Nb-Zr	Ni-O-Si
Al-B-Cr	Al-Cr-Pt	Al-Nb-O	B-Cr-Re	C-Cr-Zr	C-Ti-Zr	Co-O-W	Cr-Ni-W	Fe-Ni-O	Ni-O-W
Al-B-Hf	Al-Cr-Ta	Al-Nb-Si	B-Fe-Nb	C-Cu-Fe	C-W-Zr	Co-Re-W	Cr-Ni-Zr	Fe-Ni-W	Ni-O-Y
Al-B-Mo	Al-Cr-Ti	Al-Ni-O	B-Hf-Nb	C-Fe-Mn	Co-Cr-Mo	Co-Ti-W	Cr-O-Y	Fe-O-W	Ni-O-Zr
Al-B-Ni	Al-Cr-Zr	Al-Ni-Pd	B-Hf-Ni	C-Fe-O	Co-Cr-Nb	Co-Ti-Zr	Cr-O-Zr	Fe-O-Y	Ni-Re-Ta
Al-B-Re	Al-Cu-Fe	Al-Ni-Pt	B-Hf-Re	C-Hf-Mo	Co-Cr-Ni	Co-W-Zr	Cr-W-Zr	Fe-O-Zr	Ni-Re-Ti
Al-B-Ti	Al-Cu-Mn	Al-Ni-Re	B-Hf-Ta	C-Hf-Ni	Co-Cr-Re	Cr-Cu-Fe	Cu-Fe-Mn	Hf-Mo-Ni	Ni-Re-W
Al-B-Zr	Al-Cu-Si	Al-Ni-Si	B-Mo-Nb	C-Hf-Ta	Co-Cr-Ti	Cr-Cu-Nb	Cu-Fe-Mo	Hf-Ni-Ta	Ni-Re-Zr
Al-C-Cr	Al-Fe-Mn	Al-Ni-Ta	B-Mo-Ni	C-Hf-Ti	Co-Cr-W	Cr-Cu-Ni	Cu-Fe-N	Hf-O-Si	Ni-Ru-Ta
Al-C-Hf	Al-Fe-Mo	Al-Ni-Ti	B-Mo-Re	C-Hf-W	Co-Cu-Fe	Cr-Cu-Si	Cu-Fe-Nb	Mn-O-Si	Ni-Ta-W
Al-C-Mo	Al-Fe-Ni	Al-Ni-V	B-Nb-Re	C-Hf-Zr	Co-Cu-Nb	Cr-Cu-Ti	Cu-Fe-Si	Mn-O-W	Ni-W-Zr
Al-C-Ni	Al-Fe-O	Al-Ni-W	B-Ni-Re	C-Mo-Ni	Co-Cu-Ni	Cr-Fe-N	Cu-Fe-Ti	Mn-O-Y	O-Si-Ti
Al-C-Ta	Al-Fe-Ti	Al-O-Si	B-Ni-Ta	C-Mo-Ta	Co-Cu-Ti	Cr-Fe-Ni	Cu-Fe-V	Mo-Nb-Ni	O-Si-Y
Al-C-Ti	Al-Hf-Mo	Al-O-Y	B-Re-Ta	C-Mo-Ti	Co-Fe-Nb	Cr-Fe-O	Cu-Mn-Ni	Mo-Ni-O	O-Si-Zr
Al-C-W	Al-Hf-Ni	Al-O-Zr	B-Re-Ti	C-Mo-Zr	Co-Fe-O	Cr-Fe-W	Cu-Mn-Si	Mo-Ni-Re	O-Y-Zr
Al-C-Zr	Al-Hf-O	Al-Ru-Ti	B-Re-W	C-N-Ta	Co-Fe-Ti	Cr-Hf-Nb	Cu-Mo-Ni	Mo-Ni-Ti	Re-Ta-W
Al-Co-Cr	Al-Hf-Re	Al-Ta-Ti	C-Co-Cr	C-Nb-Re	Co-Mn-O	Cr-Mn-N	Cu-Ni-Si	Nb-Ni-W	Re-W-Zr
Al-Co-Fe	Al-Hf-Ta		C-Co-Hf	C-Nb-W	Co-Mo-Ta	Cr-Mo-Ni	Cu-Ti-Zr	Nb-O-Si	Ta-W-Zr
Al-Co-Hf	Al-Hf-Ti		C-Co-Mo	C-Ni-Ti	Co-Mo-W	Cr-Nb-Ni	Fe-Mn-N	Nb-Re-Ta	Ti-W-Zr
Al-Co-Mo	Al-Hf-W		C-Co-Ti	C-Ni-W	Co-Ni-Re	Cr-Nb-Si	Fe-Mn-Ni		
Al-Co-Ni	Al-Hf-Zr		C-Co-W	C-Ni-Zr	Co-Ni-Ru	Cr-Ni-Re	Fe-Mo-Ni		
Al-Co-O	Al-Mn-Ni		C-Co-Zr	C-Re-W	Co-Ni-Ta	Cr-Ni-Ru	Fe-Mo-W		
Al-Co-Ta	Al-Mn-O		C-Cr-Hf	C-Ta-Ti		Cr-Ni-Si	Fe-Nb-Ni		
Al-Co-Ti	Al-Mn-Si		C-Cr-Ni	C-Ta-W		Cr-Ni-Ta			
Al-Co-W	Al-Mn-Ti		C-Cr-Re	C-Ta-Zr					
Al-Co-Zr	Al-Mo-Ni		C-Cr-Ta						
Al-Cr-Hf	Al-Mo-Re		C-Cr-Ti						
Al-Cr-Ni									

272 assessed ternary systems in full range of composition and temperature

Predicting multi-component alloys

stainless steels,
carbon and low alloy steels, high-speed steels and
chromium steels
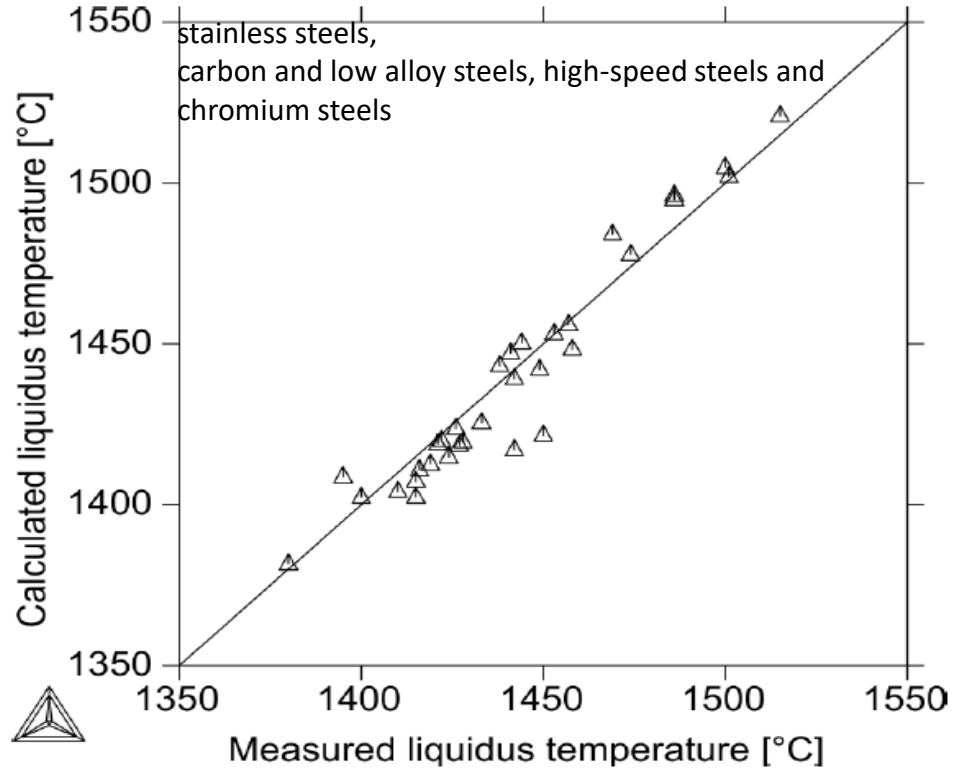
Extending to multi-component diffusion

Full consideration of the thermodynamic and kinetic influence from alloying elements like e.g. Manganese, Silicon, Chromium
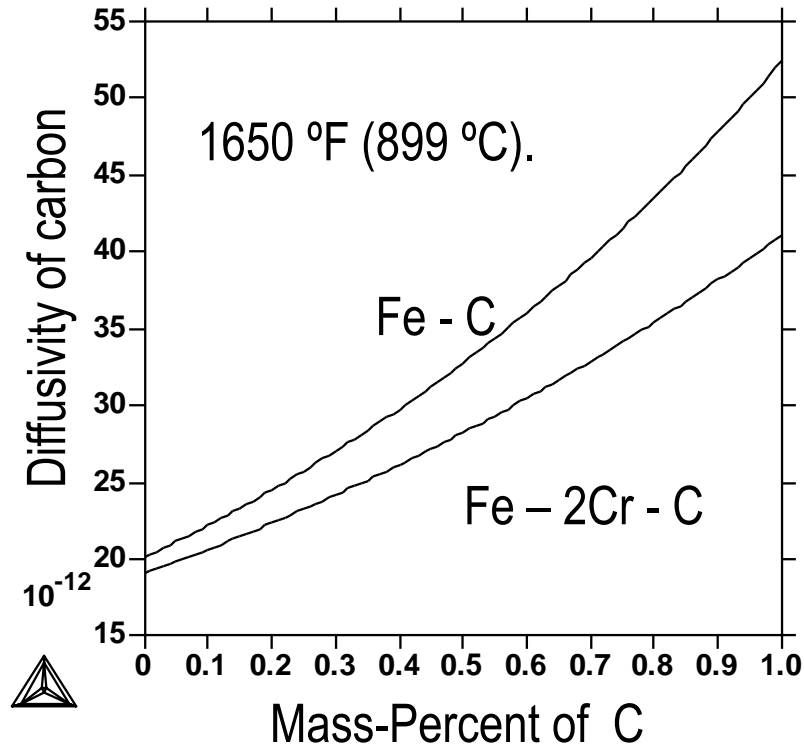
Software: An integrated approach

Thermo-Calc

Minimization of the total Gibbs free energy under given conditions.

$$G = \sum_{\phi} N^{\phi} G_m^{\phi}\left(T, P, x_i^{\phi}\right)$$

$$\frac{\partial G}{\partial x_i^{\phi}} = 0$$

DICTRA

1-D diffusion simulation - Numerically solve diffusion equations

Solve Diffusion

$$\frac{\partial \mathbf{c}}{\partial t} = -\frac{\partial}{\partial z}(\mathbf{J}) \quad \text{where} \quad \mathbf{J} = -\mathbf{D}\frac{\partial \mathbf{c}}{\partial z}$$

TC-PRISMA

Mean field precipitation simulation – using LS (Langer-Schwartz) and KWN (Kampmann and Wagner Numerical) Approach

Continuity equation

$$\frac{\partial f(r,t)}{\partial t} = -\frac{\partial}{\partial r}\left[\upsilon(r)f(r,t)\right] + j(r,t)$$

$$C_0^{\alpha} = C^{\alpha} + \left(C^{\beta} - C^{\alpha}\right)\int_0^{\infty} \frac{4\pi}{3} f(r,t)r^3 dr$$

Mass balance

What can be predicted?

Thermo-Calc

- Stable/Metastable Equilibria
- Amount and composition of phases
- Transformation temps (liquidus, solidus, A1, A3, solvus, Ms etc)
- Density/Thermal expansion
- Solidification segregation
- Enthalpy, heat capacity, latent heat etc.
- Phase diagrams

DICTRA

- Carburizing and decarburization
- Microsegregation during solidification
- Homogenization treatment
- Precipitate growth and dissolution
- Precipitate coarsening
- Interdiffusion in coating/substrate systems
- TLP bonding of alloys (brazing)

TC-PRISMA

- Particle Size Distribution
- Number Density
- Average Particle Radius
- Volume Fraction
- TTT/CCT
- Average Compositions
- Interface Compositions
- Nucleation Rate
- Critical Radius

Composition/process – structure link I

❑ The most rudimentary assumption would be to assume full equilibrium.

❑ No specific consideration of the process.

❑ Predict phase transformation temps.

❑ Volume fractions of phases (and composition)

❑ Thermodynamic properties (e.g. Cp)
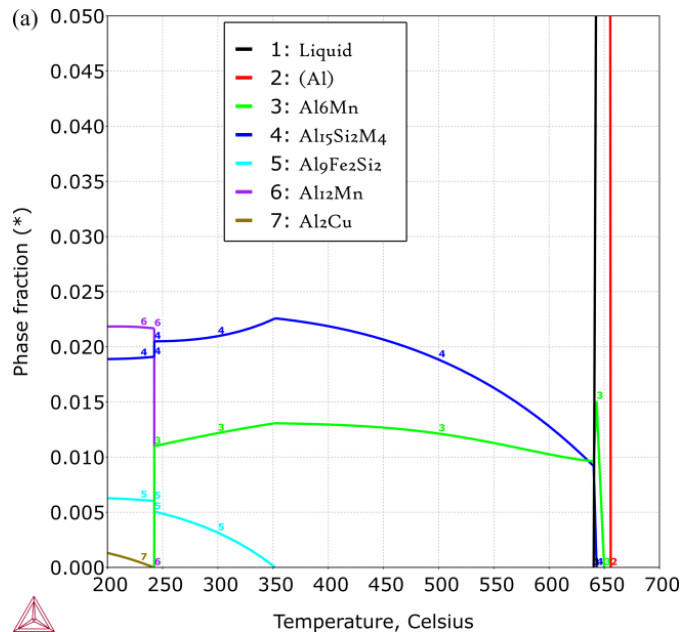
Phase stability as function of Temp for alloy 3003
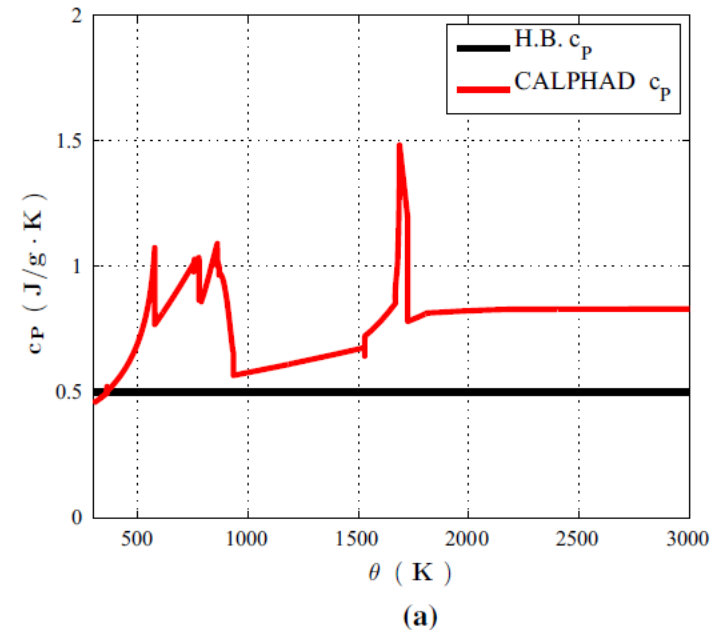
Comparison of handbook values and CALPHAD calculated values of Cp – from Smith, et al. / Computational Mechanics 57.4 (2016): 583-610.

Composition/process – structure link II

❑ Next step is to account for kinetics, i.e. non-equilibrium processes.

❑ Some consideration of the process, e.g. temperature-time evolution.

=> Allows us to predict non-equilibrium states and some geometrical aspects, e.g. precipitate size and distribution.
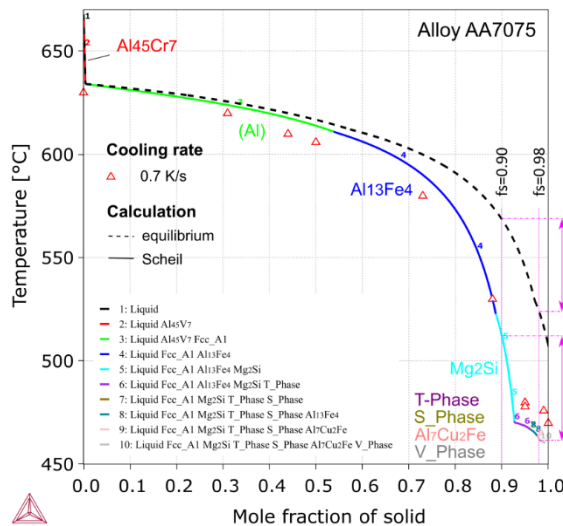
Non-eqm solidification
of alloy AA7075
CASTING
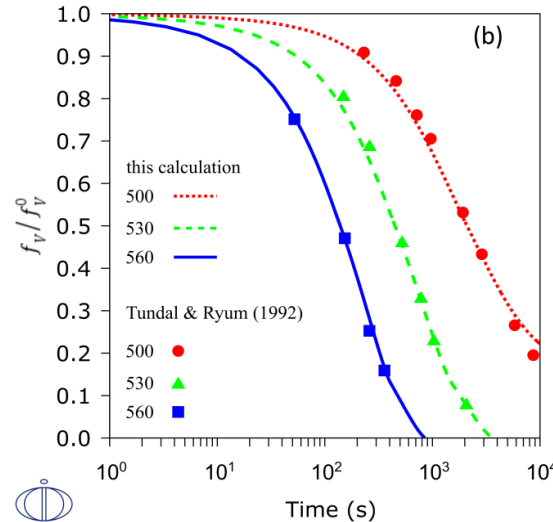
Dissolution of particles

HOMOGENIZATION
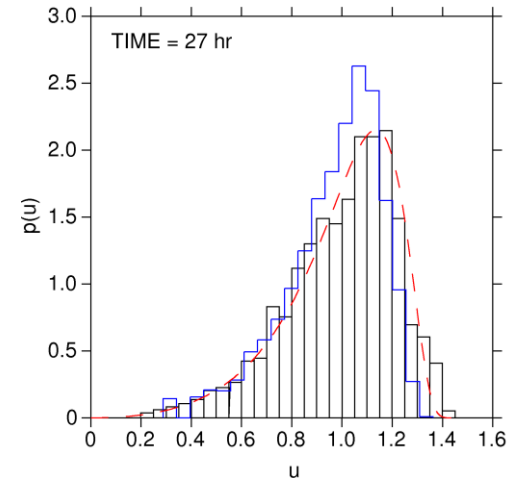
Size distribution of precipitates

ANNEALING / AGING

Homogenizing

The production of most alloys, including wrought ones, starts with melting and casting.

The goal of homogenization is to provide uniformity in composition through dissolution of certain phases formed during solidification or normalizing chemical inhomogeneities arising from micro-segregation during solidification.

Casting and Solidification: Approaches to modeling

The manufacturing of most alloys, including wrought ones, starts with melting and casting.

- **To understand and predict**
  - Solidified microstructures
  - Phase formation (sequence)
  - Phase reactions
  - Microsegregation during solidification which leads to inhomegeneity
  - Latent heat of evolution
  - Volume change/shrinkage

- **Solidification simulations**
  - Equilibrium stepping calculation
  - Scheil simulation
  - Mixed Scheil simulation

- **Assumptions in Scheil**
  - Diffusion in solid phases is negligible
  - Liquid is assumed to be homogeneous
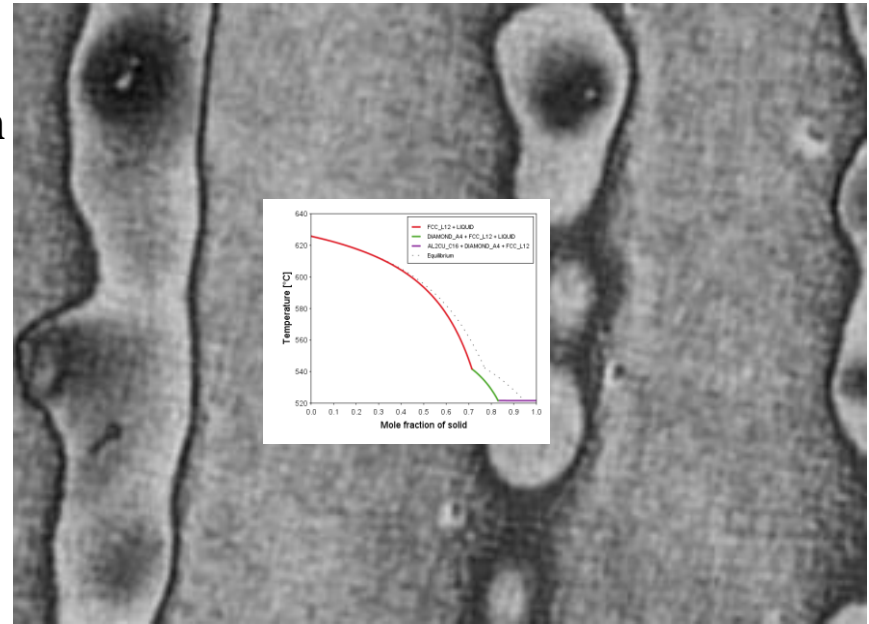
Homogenization: Dissolution of precipitates (I)

- **Homogenization of (Al) matrix**
- **Dissolution of GB particles (α-Al$_{15}$Si$_2$Mn$_4$, β-Al$_9$Fe$_2$Si$_2$, π, Mg$_2$Si and Si)**
- AA6005 alloy (Al-0.82Si-0.55Mg-0.016Cu-0.5Mn-0.2Fe, wt. %)
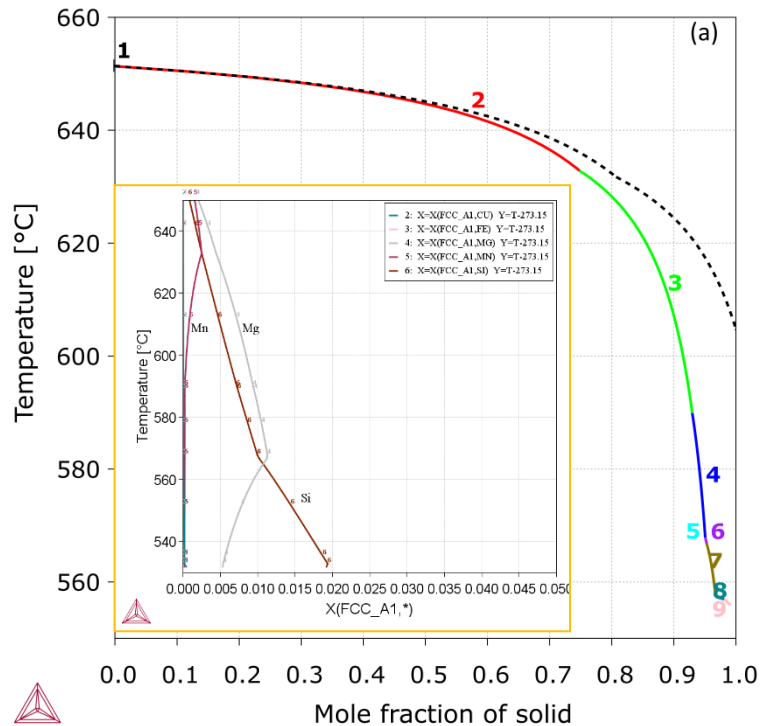
Scheil simulation
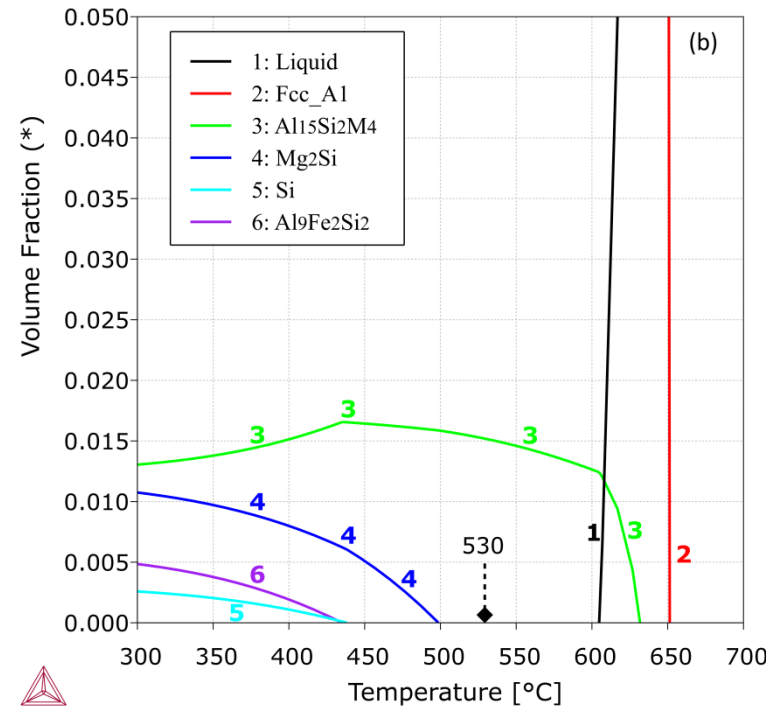
Equilibrium calculation

Homogenization: Dissolution of precipitates (II)

- Homogenization of (Al) matrix
- Dissolution of GB particles

- Temperature? time?

- DICTRA simulations, TCAL5 + MOBAL4

- Single particle
- Multi-cells approach
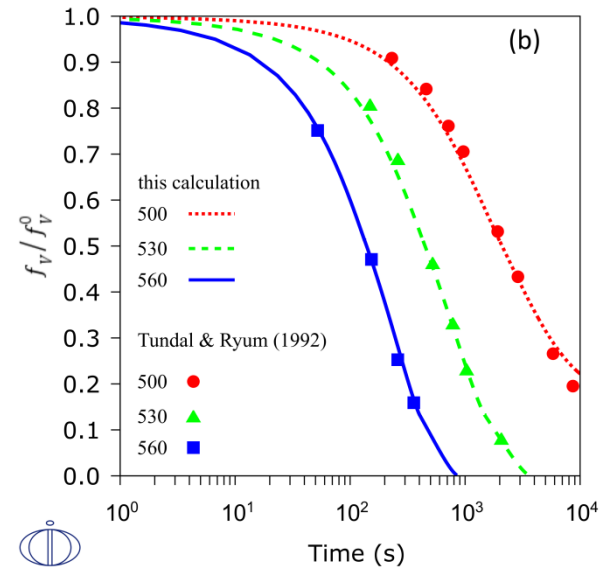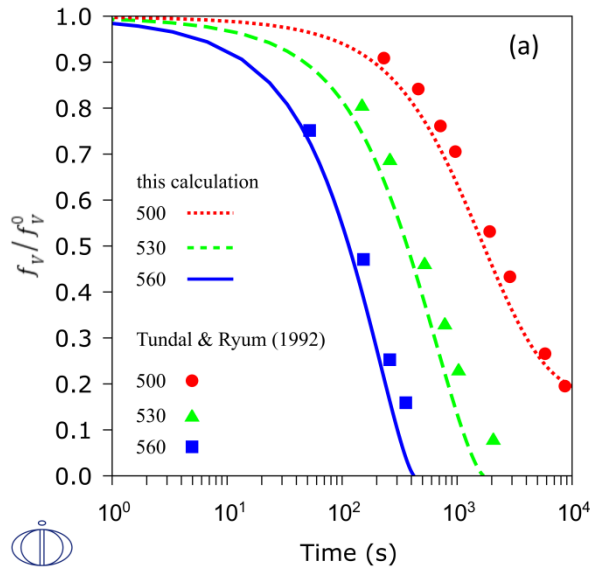
Dissolution of Si particles at 500 °C, 530 °C, and 560 °C
L: single particle; R: multiple-cell approaches (particle size distribution)

Homogenization: Homogenizing compositions (I)

Homogenizing a Nickel based superalloy: Thermodynamic and kinetic simulation and experimental results.
Paul D Jablonski and Christopher J Cowen (NETL, Albany, OR)
Met. Trans. B. Vol 40B, April 2009 (pp 182-186)

Table I. Target and Measured Chemistry (in Weight Percent) of the Nimonic 105 Alloy Cast for This Study

Nimonic 105	C	Cr	Mo	Co	Al	Ti	Mn	Si	B
Target	0.15	14.85	5	20	4.7	1.1	0.5	0.5	0.05
Measured	0.16	14.61	5.02	20.04	4.43	1.1	0.51	0.51	0.05

Scheil calculation
used to predict the fraction solid
curve and incipient melting
temp -1142°C.

and extent of chemical
microsegregation - amounts of each
alloying element in the FCC (γ) phase
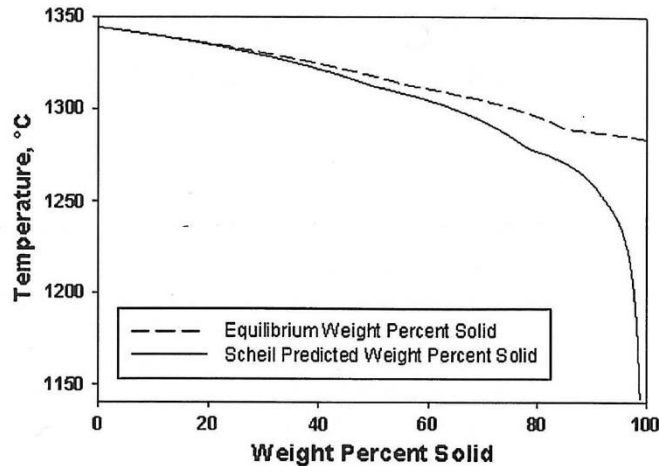
Fig. 1—Equilibrium and Scheil predicted solidification ranges for the Nimonic 105 alloy.

MC carbide forms

Carbides MC & M_6C lose stability
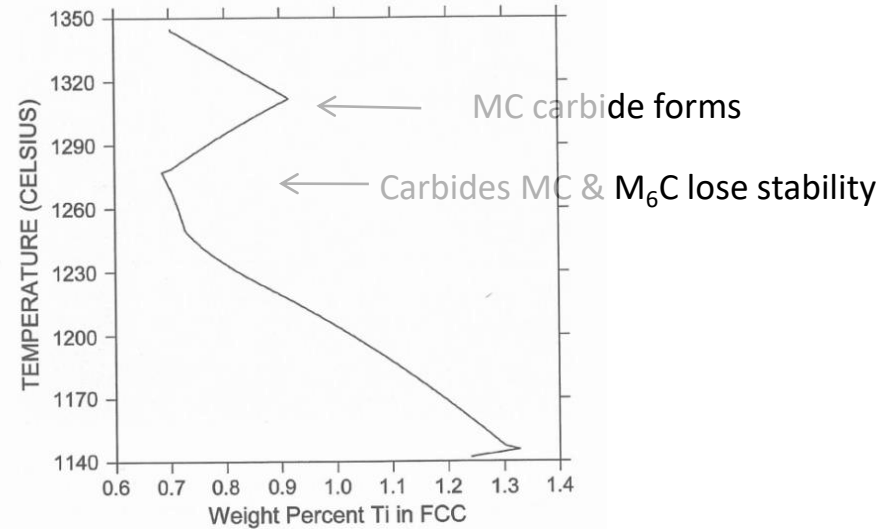
Fig. 2—Calculated amount of Ti in the fcc phase as a function of temperature.
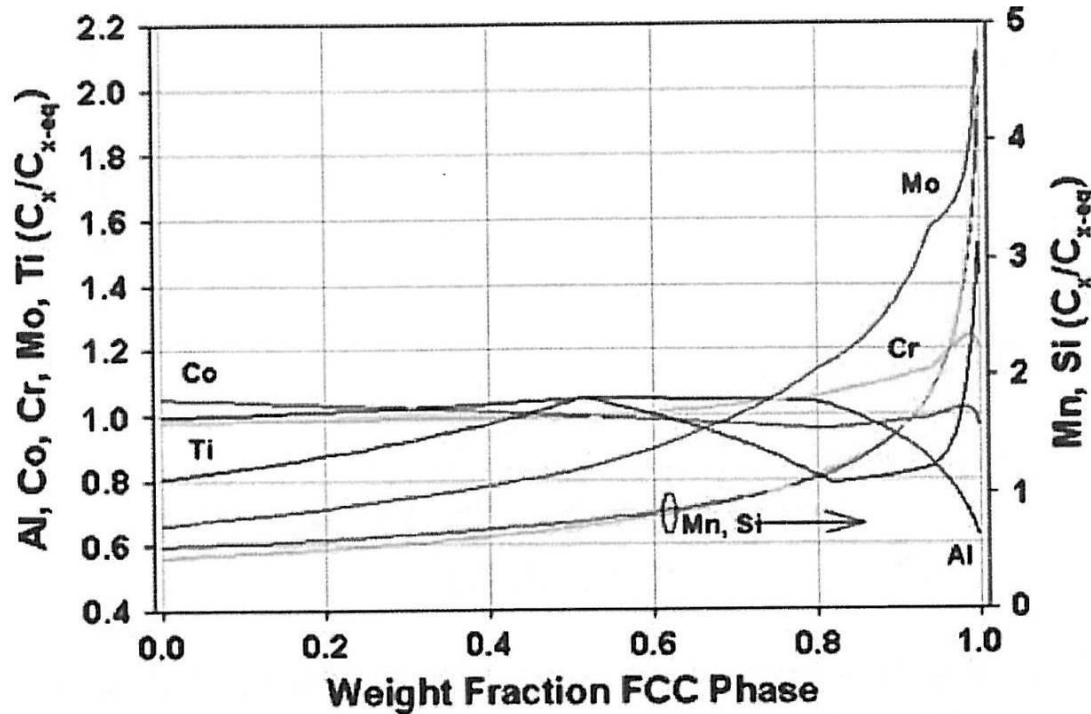
Fig. 3—Normalized Scheil predicted segregation across a dendrite (from center to edge).

Homogenization: Homogenizing compositions (IV)

Thermo-Calc Software

DICTRA simulations performed to simulate homogenization.

Assumptions: Diffusion distance of 50 mm based on approx one half of the maximum secondary dendrite arm spacing. Weight fraction of FCC scaled to this distance and read into DICTRA along with the chemistry profiles across the FCC dendrites from the Scheil simulations.
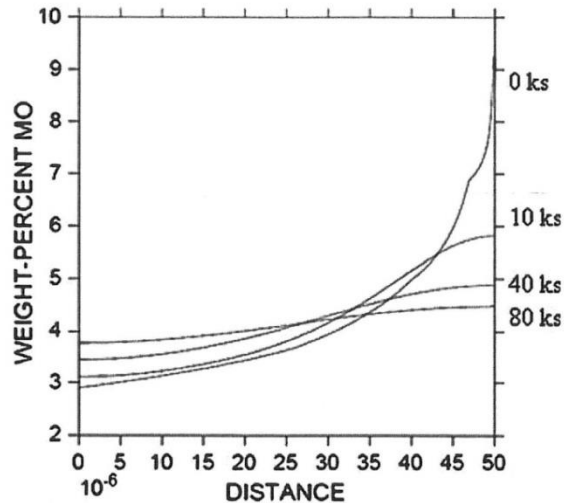
Fig. 4—Weight percent Mo as a function of distance (m) across a dendrite (from center to edge) for the following time sequences at 1100 °C: 0, 10, 40, and 80 ks.
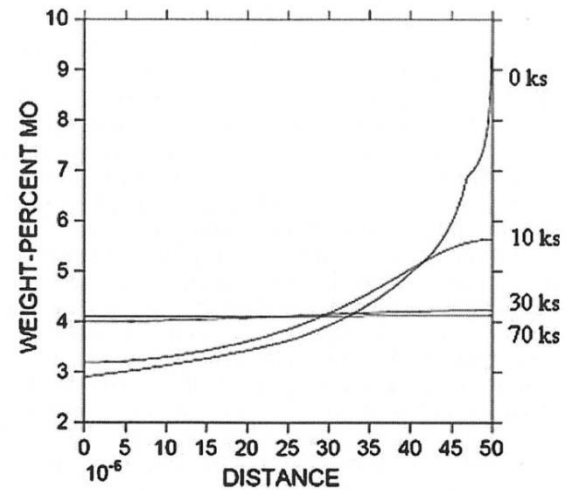
Fig. 5—Weight percent Mo as a function of distance (m) across a dendrite (from center to edge) for the following time sequences at 1100 °C: 0 and 10 ks; and 1100 °C/10 ks + 1200 °C/30 and 70 ks.

First heat treatment simulated at 1100°C (below incipient melting temp).

But incipient melting temp changes with chemical profile. In second case calculated a new incipient melting temp after 10,000 secs of 1275°C.

Significant improvement of the alloy homogeneity was predicted even after only 8.33 hrs (30,000 secs) @1200°C after the initial 10,000 secs @ 1100°C.

Annealing / Aging

Annealing is performed to produce desired changes in the microstructure with the goal of engineering certain properties, e.g. precipitate strengthening, grain pinning etc.

Phase diagrams: Heat treatment windows

Example: Nitrogen in HSLA Steel Fe-1.5Mn-0.3Si-0.1V-C (wt%)
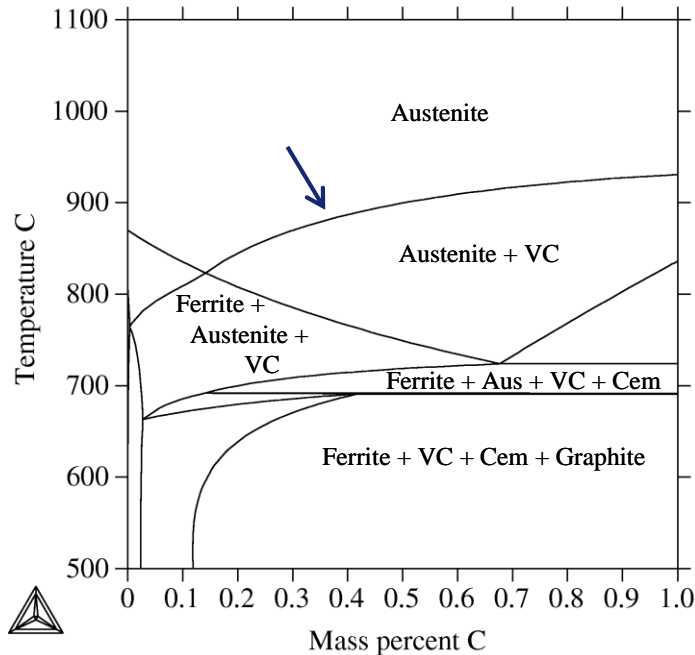
1. No nitrogen present
Heat treatment above 850 - 900ºC may lead to grain growth for steels with normal carbon content
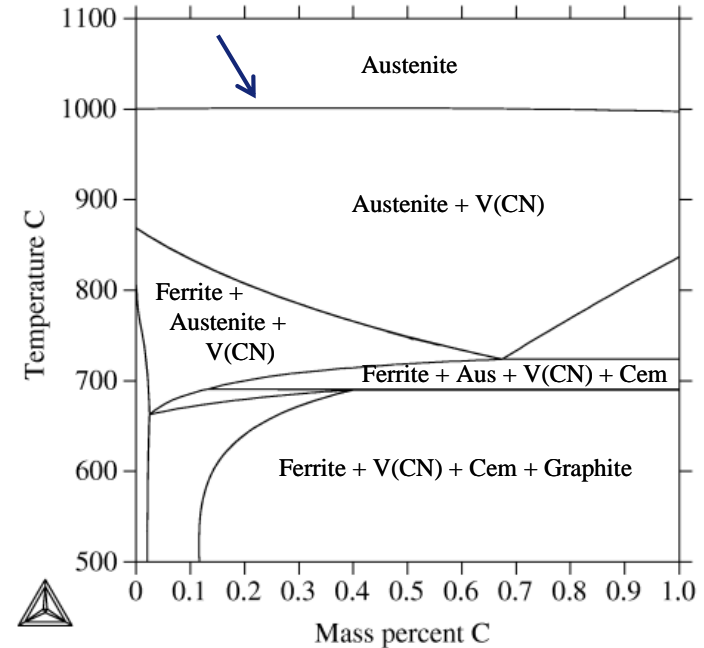
2. With the addition of only 0.003 wt-% N.
The two phase field of austenite + V(C,N) is much extended, and grain growth can be avoided up to 1000ºC. The phase diagram at low T is not much altered compared to 1.

TTT diagrams for precipitate phases

System	
Database package	TCFE9 + MOBFE4
Elements	Fe,C,Cr,Mn,Ni,Si
Matrix phase	Fcc_A1
Precipiate phase	$M_{23}C_6$

Conditions – TTT diagram	- **Phase fraction = 0.0005**
Composition	Fe-0.068C-20.89Cr-1.61Mn-10.28Ni-0.49Si (wt.%)
Temperture	500 °C, 800 °C, 20 °C
Simulation time	1E8 s
Nucleation properties	Nucleation Site Type: Grain Boundary, Grain size 100 μm

Data Parameters	
Interfacial Energy	Grain Boundary: 0.18 J/m^2
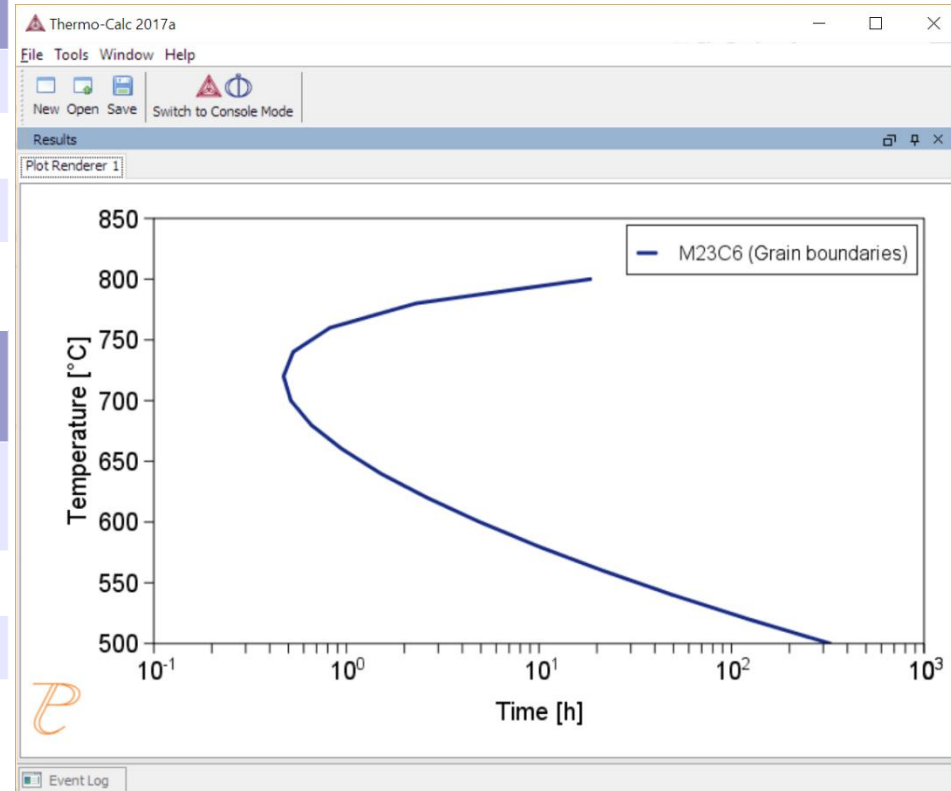
Precipitate size distribution

TC-PRISMA simulation of precipitation kinetics of M23C6 in AISI 316.
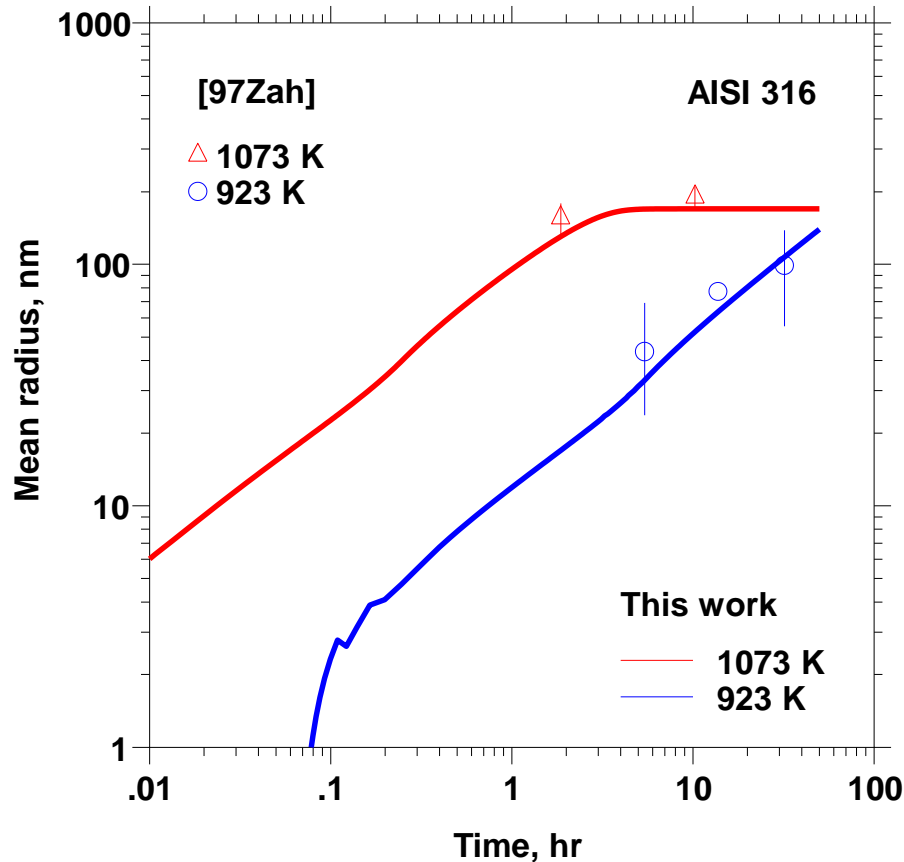
Input data for simulation:

❑Thermodynamic & kinetic data

❑Composition
    C 0,08%
    Cr 18%
    Ni 12%
    Mo 2%
    Mn 1.5%

❑Time & temperture

❑Nucleation at grainboundaries

@ 650 °C

• γ-grainsize =100 μm

□σ = 0.3 J/m^2

@ 800 °C

• γ-grainsize =1000 μm

□ σ = 0.2 J/m^2

Long term microstructure stability

P91:   Fe-0.09C-0.29Si-0.35Mn-8.70Cr-0.90Mo

P92:   Fe-0.106C-0.04Si-0.46Mn-8.96Cr-0.47Mo-1.84W

Consider $M_{23}C_6$ only, ignore MX and Laves phase

σ = 0.36 J/m^2

Non-isothermal:
Austenitisation at 1050 ºC

Tempering at 765 and 770 ºC

Long term creep rupture test at 650 ºC

Hald & Korcakova, ISIJ International,
43(2003)420-427
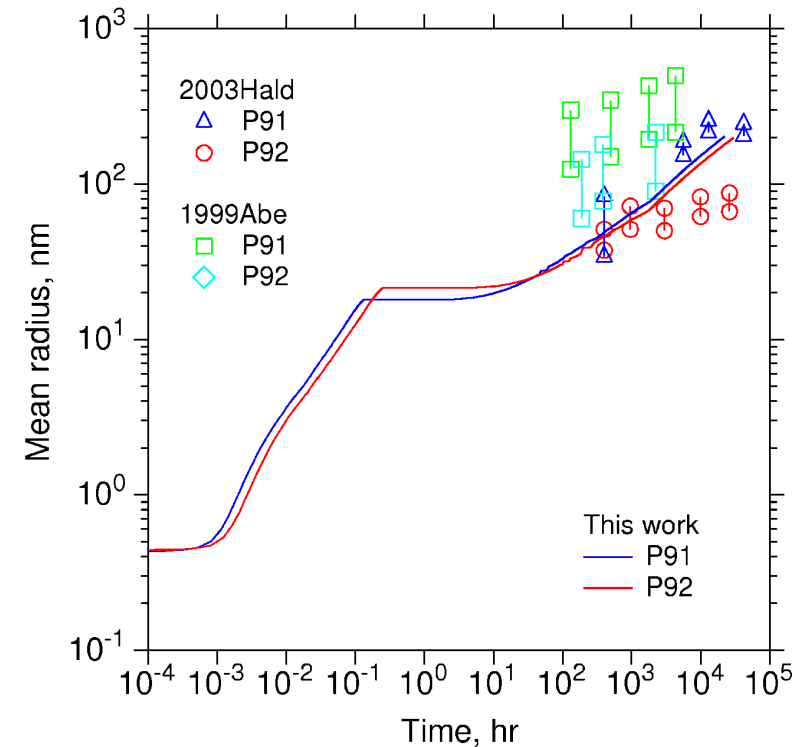
Aging treatment AA6005

- **TC-PRISMA precipitation simulation**
- β'' & Al-containing β'' > β'' with Al solubility
- Sphere > needle

- Strain, $\varepsilon_{11} = 0.06$, $\varepsilon_{22} = 0.06$, $\varepsilon_{33} = 0.0007$
- Interfacial energy, 0.099 J/m^2

Chen et al. Mater. Today Proc. 2 (2015) 4939.
Chen et al. CALPHAD, 62 (2018) 154-171.
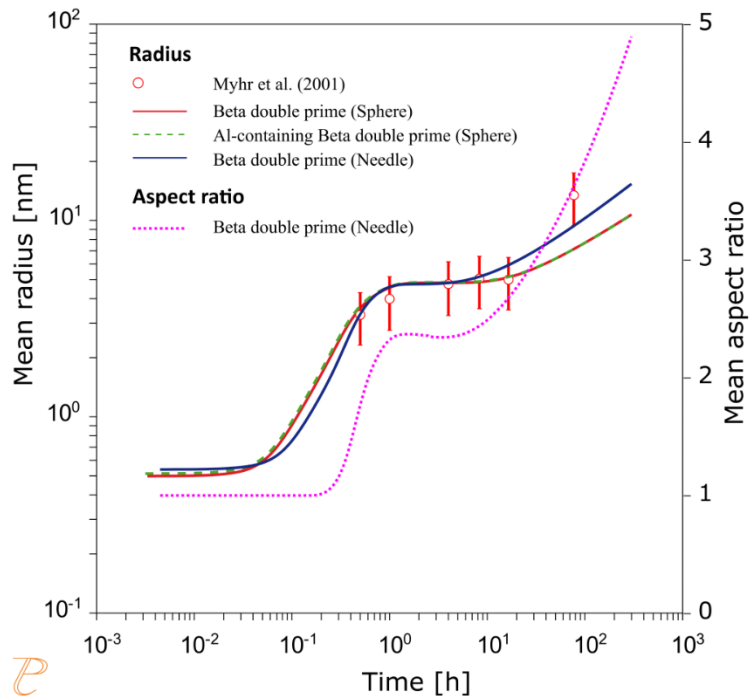
Simulated mean radium and aspect ratio of β'' precipitates in AA6005
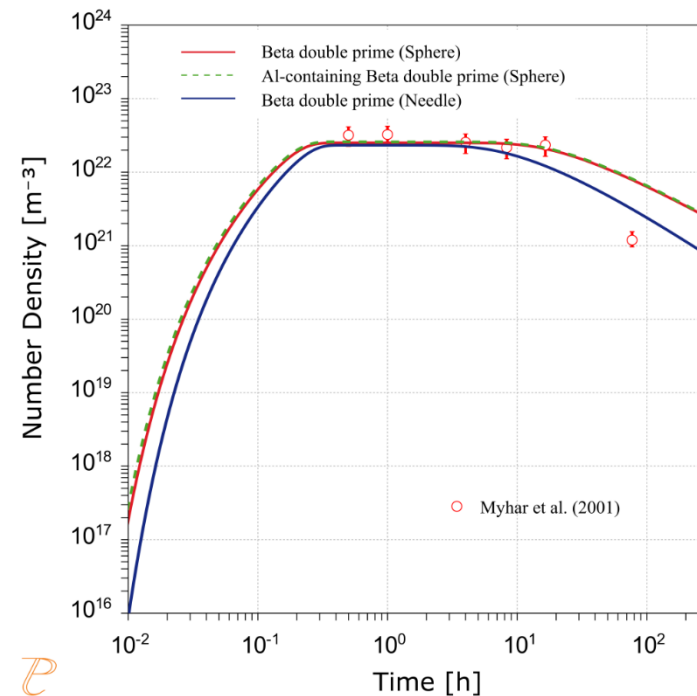
Simulated number density of β'' precipitates in AA6005 alloy at 185 °C

Input to yield strength models

Danielle B. Cote et al.(WPI), TMS 2016

E.g. Al 2024
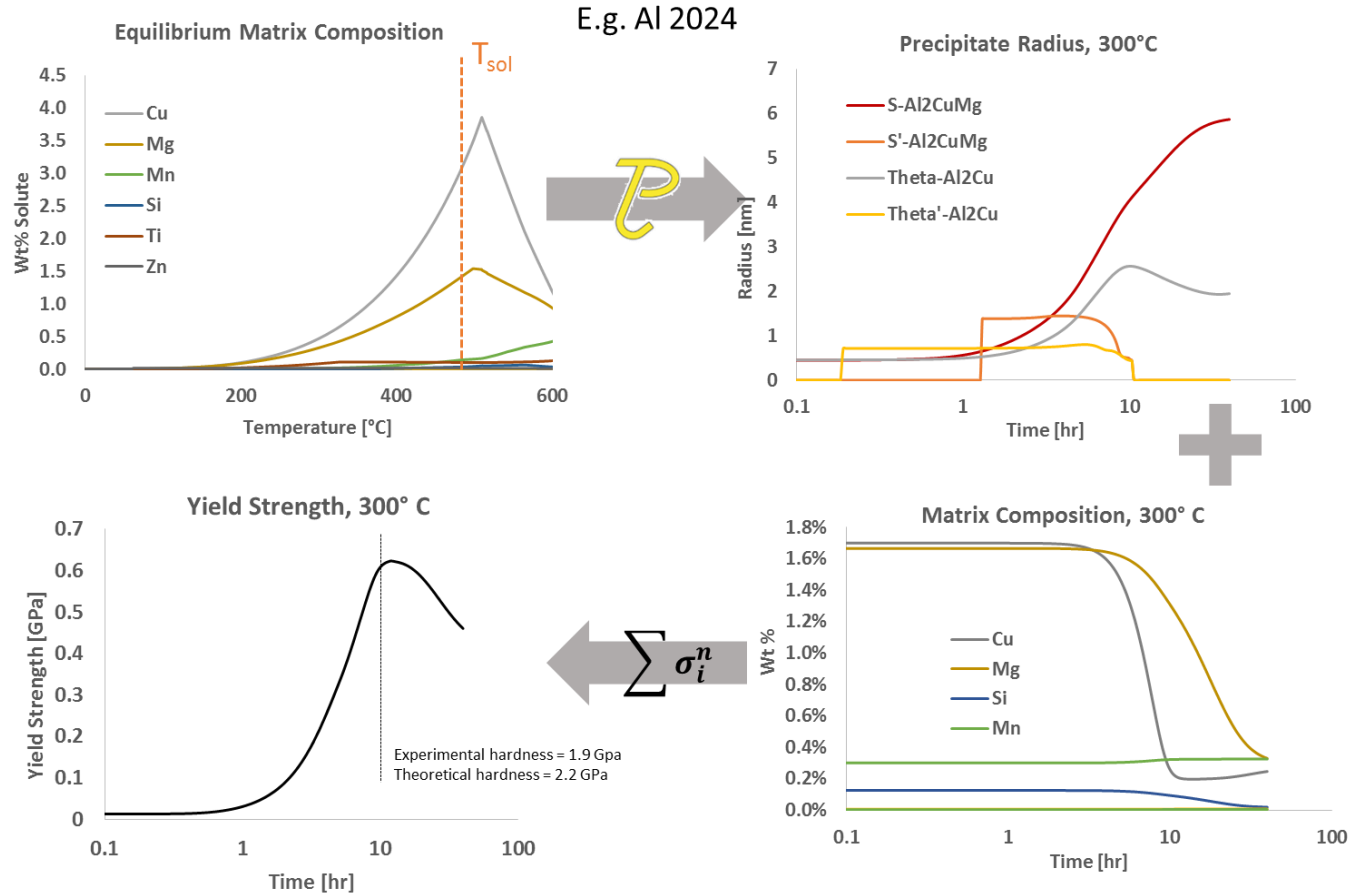
Surface hardening

Gas carburizing, nitriding, ferritic nitrocarburizing and carbonitriding are several surface hardening processes which are used to impart a hard wear resistant surface to parts while maintaining a softer, tougher interior.

Calculating Low pressure decomposition of gases (I)

Bulk Compositions:
- ❖ Pure Propane;

- ✓ Conditions:
  - ➤ Constant pressures, 100 mbar (temperature 400 - 1000°C);
  - ➤ Constant temperature, 950°C (pressure 0.01 – 1000 mbar).

- ✓ Constrains:
  - ➤ Graphite suspended (formation of graphite prohibted);
  - ➤ Graphite present (formation of graphite considered).

Calculating Low pressure decomposition of gases (II)

Thermo-Calc Software

Decomposition of Propane at 100 mbar and various temperatures
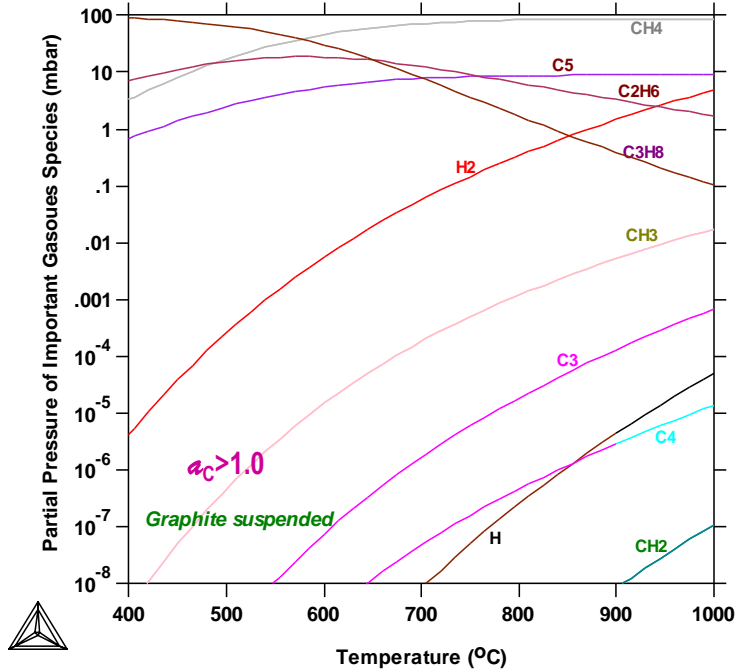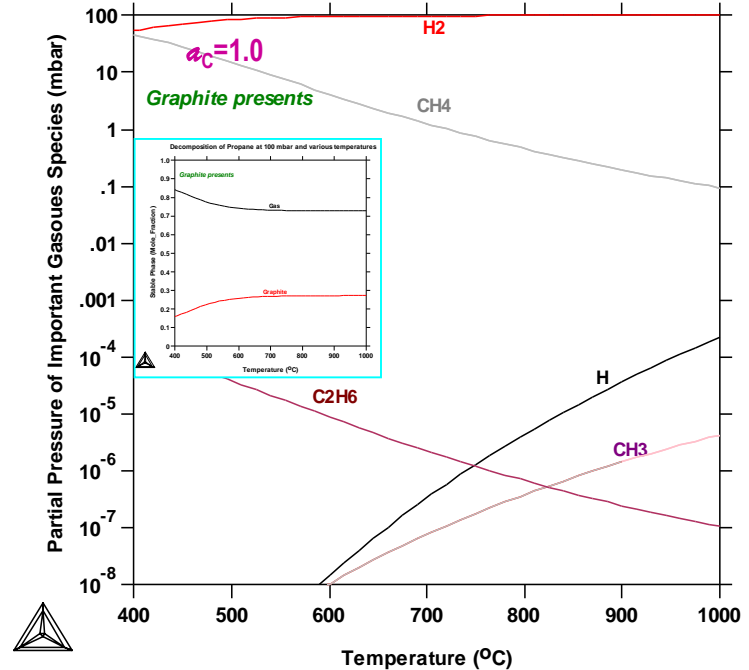
Gas speciation resulted from propane decomposition at 100 mbar and various temperatures, in a system where graphite formation is prohibited.

Gas speciation and stable phase amounts during propane decomposition at 100 mbar and various temperatures, in a system where graphite formation is possible.

Calculating Low pressure decomposition of gases (III)

Thermo-Calc Software

Decomposition of Propane at 950 C and various pressures
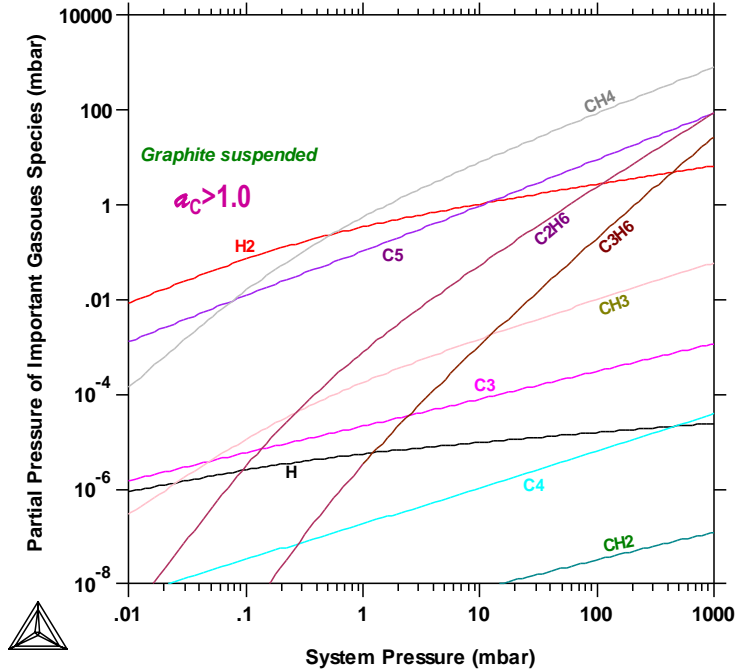
Gas speciation resulted from propane decomposition at 950°C and various pressures, in a system where graphite formation is prohibited.

Decomposition of Propane at 950 C and various pressures
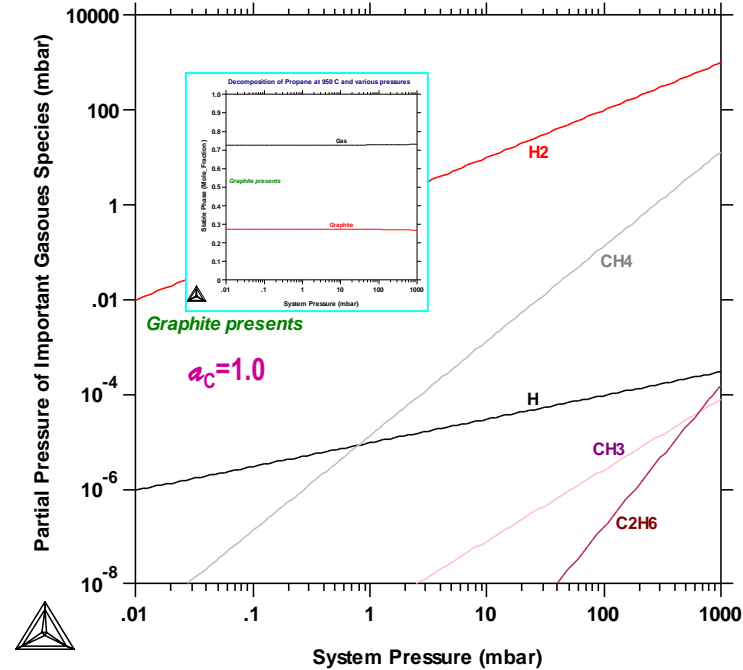
Gas speciation and stable phase amounts during propane decomposition at 950°C and various pressures, in a system where graphite formation is possible.

Calculating critical potentials for control of nitriding / nitrocarburizing

Activity to potential	Partial Pressure	Process
$a_N = K_1 * K_N$	$K_N = pNH_3/p^{1.5}H_2$	Nitriding
$a_C = K_2 * K_{CB}$	$K_{CB} = p2CO/pCO_2$	
$a_C = K_3 * K_{CW}$	$K_{CW} = pH_2 * pCO/pH_2O$	Nitro-carburizing
$a_C = K_4 * K_{C-O2}$	$K_{C-O2} = pCO/P^{0.5}O_2$	
$a_C = K_5 * K_{C-CH4}$	$K_{C-CH4} = pCH_4/p^2H_2$	
	$K_O = pH_2O/pH_2$	
$a_O = K_6 * K_O$		Oxi-nitriding / postoxidizing

New measuring and control systems for ntriding and nitrocarburizing. **Winter, K-M., Torok, P***.,*
Industrial Heating, Sep 2010, pp. 61-68.

Predicting phase stability vs temperature
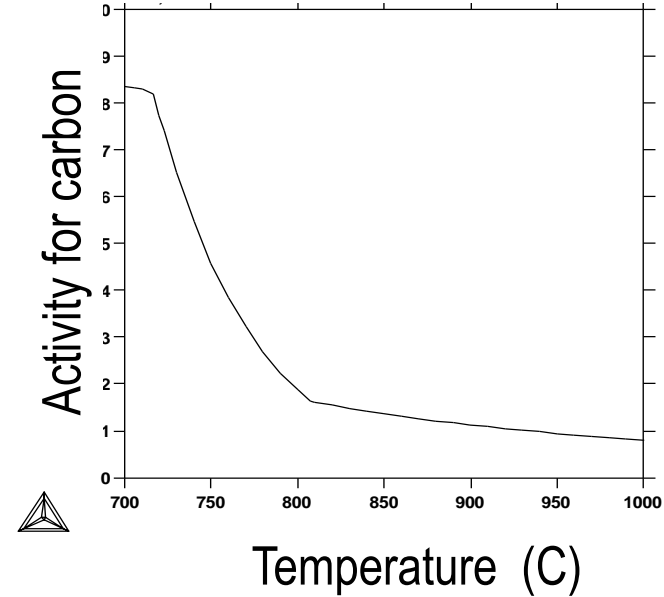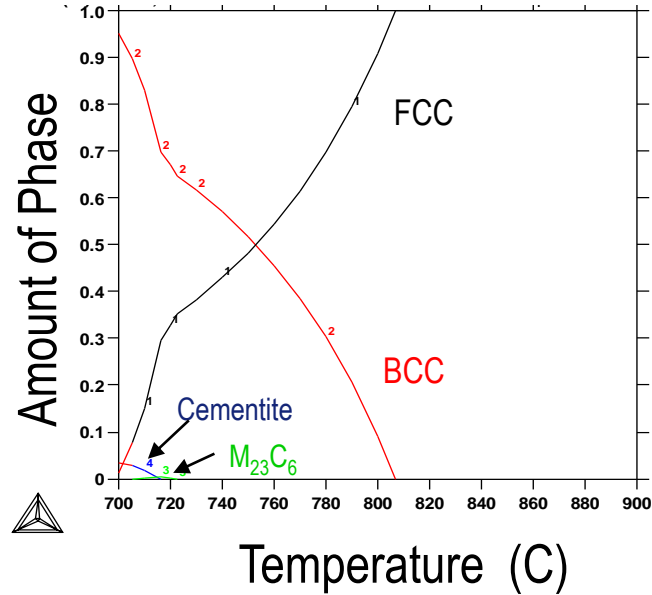
Predicting the influence from **temperature** for an AISI 8620 steel

Fe-0.5Cr-0.2C-0.8Mn-0.2Mo-0.55Ni-0.25Si

Calculating Lehrer diagram for AISI 4140 Steel
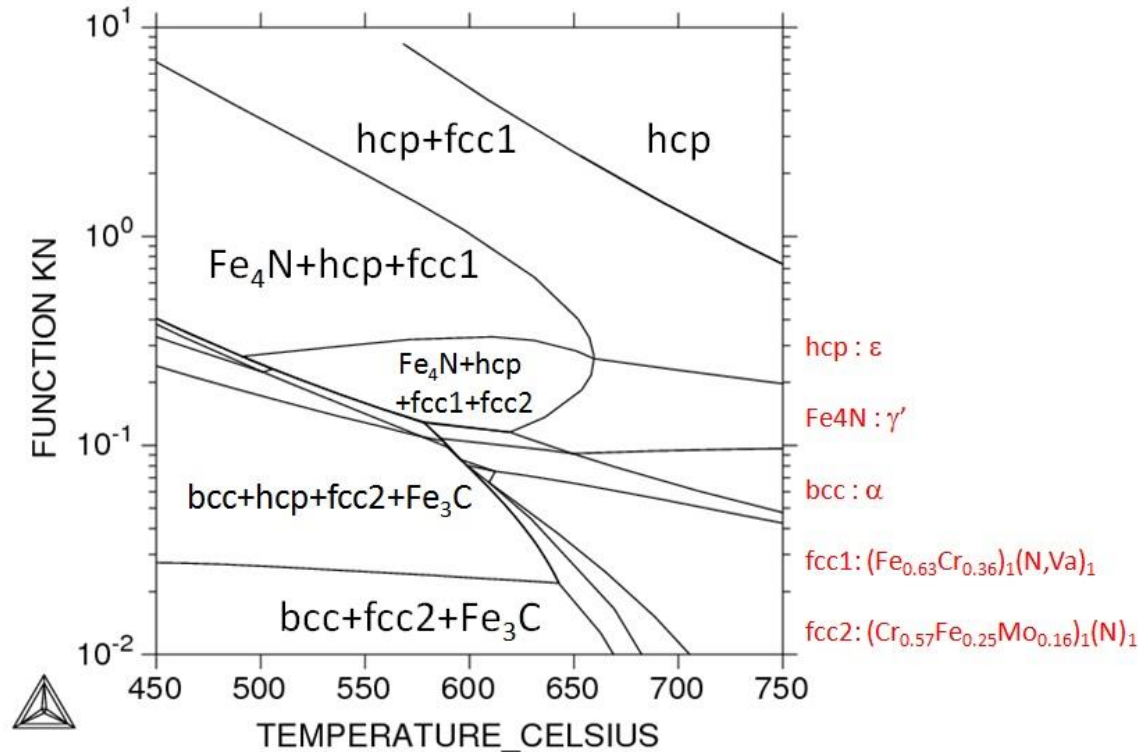
Simulating carburization (I)

Simulation of carburization of martensitic stainless steel

*Turpin et al., Met. Trans. A **36**(2005), pp. 2751-60*

Fe-12Cr-2Ni-2Mo-0.12C at 955°C:

Calculated carbon profile at the end of the enrichment step

Calculated carbon profile after 3h of diffusion

2.60 m

Fe-13Cr-5Co-3Ni-2Mo-0.007C

1750 °F (955 °C)

$J_c = 9.1 \cdot 10^{-9} (0.9 - a_c^{surf})$

2.5h

0.5h

Mass-Percent of C

Distance from surface [mm]
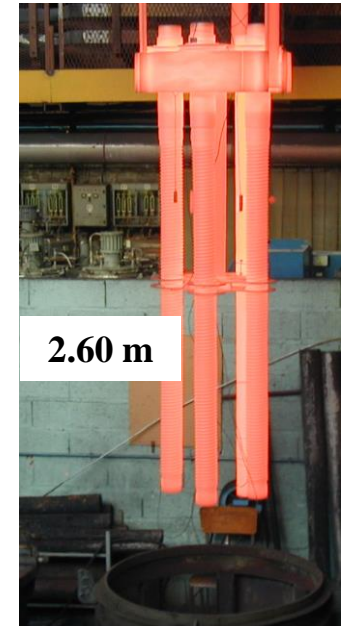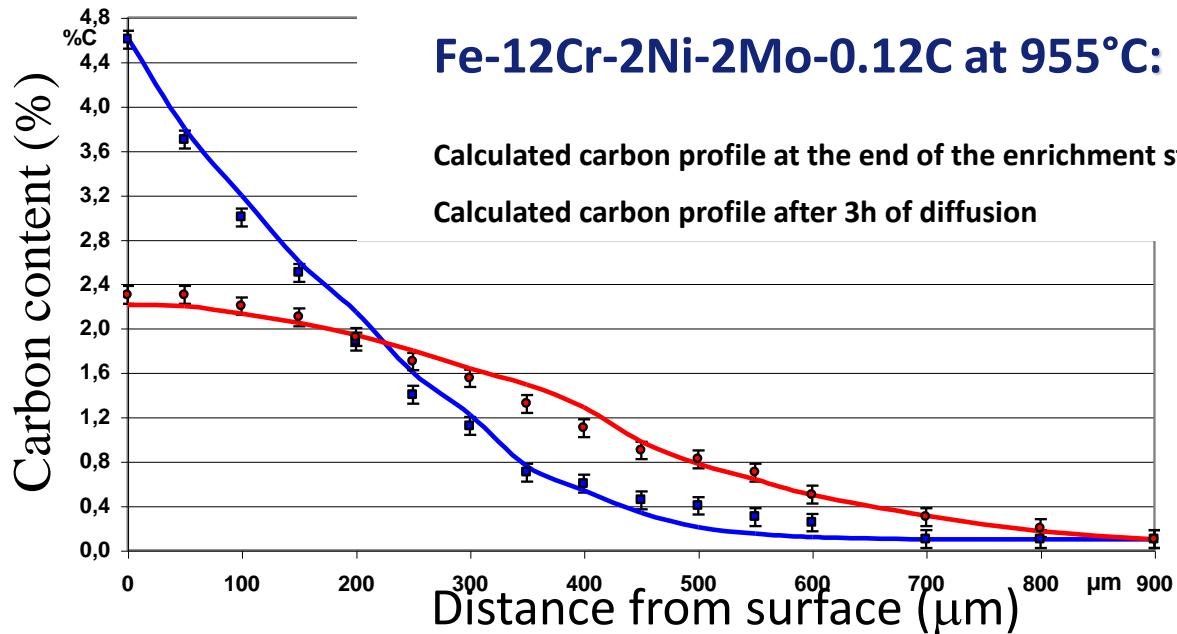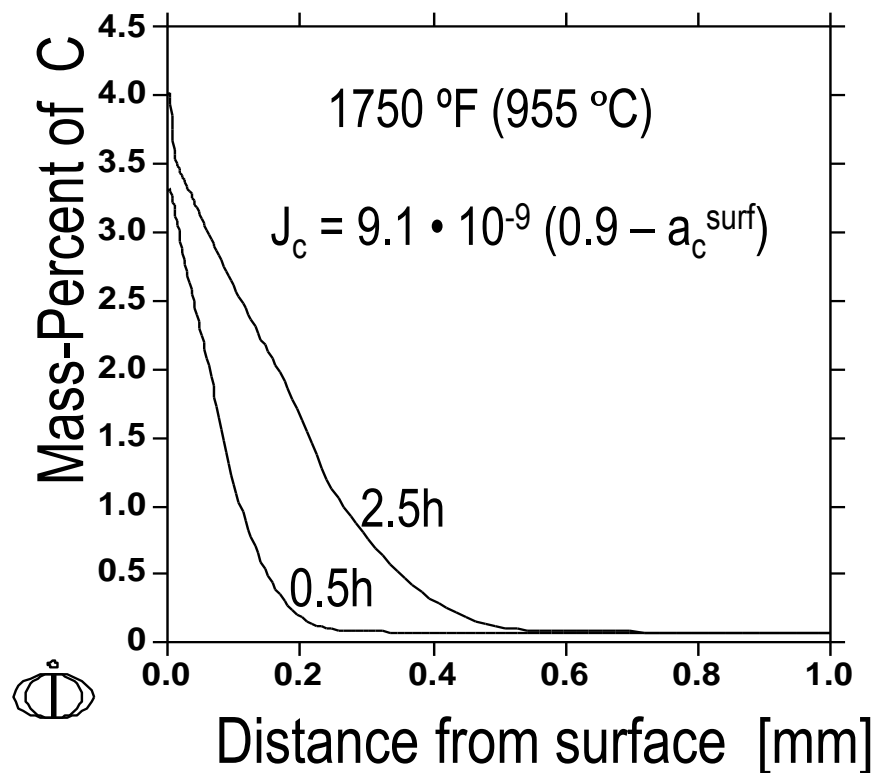
Simulating carburization (III)

Thermo-Calc Software

Carbide formation

Carbide dissolution

Left plot labels: Fraction of carbide (y-axis), Distance from surface [mm] (x-axis), M_7C_3, cem, $M_{23}C_6$, after 2.5h

Right plot labels: Mass-Percent of C (y-axis), Distance from surface [mm] (x-axis), 2.5 h, 2.5h + 1.5h

Stress relief

Stress relief temperatures
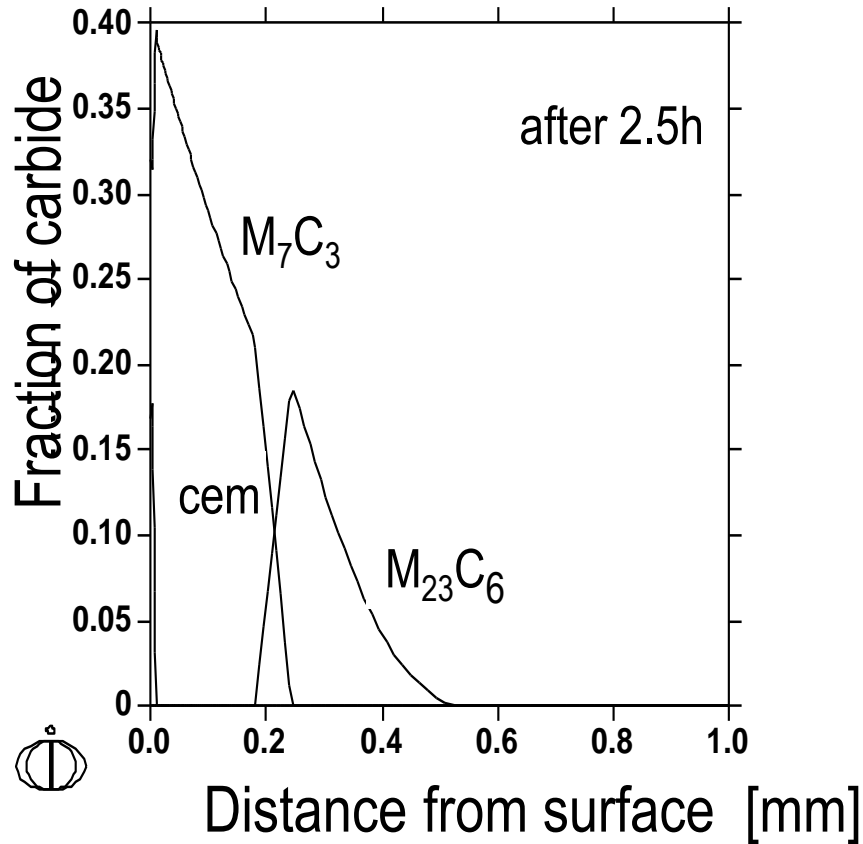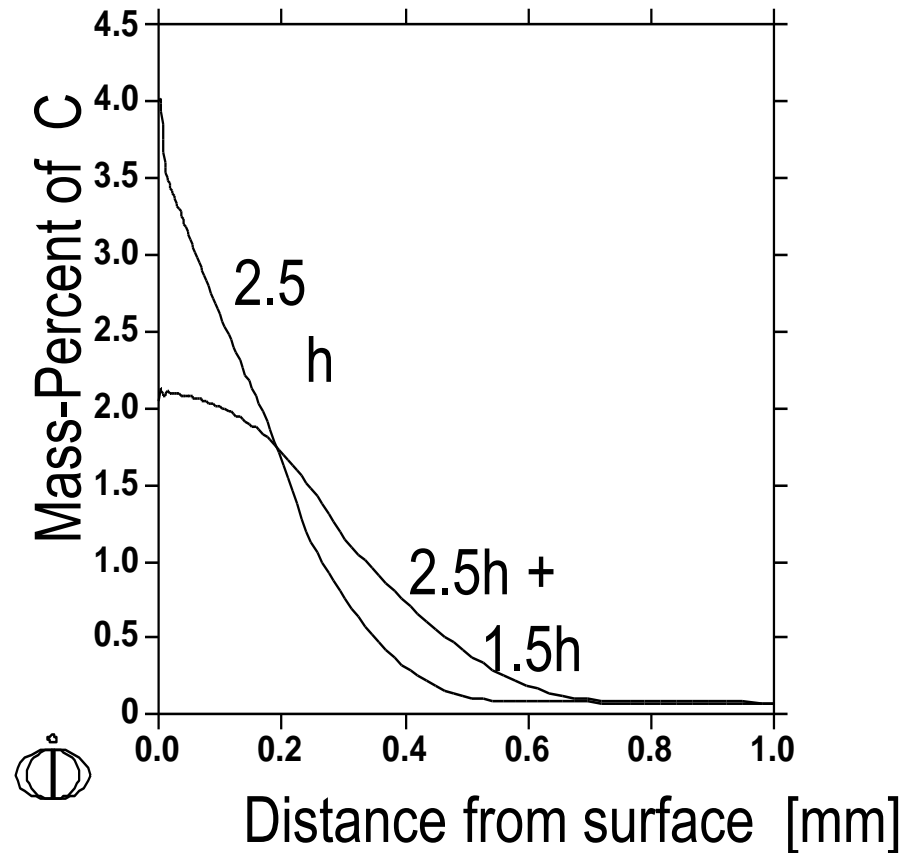
Thermo-Calc does not model distortion or residual stress. This can be done using a finite element code.

But these codes rely on good materials property data to make accurate simulations and this data is not always available from handbooks or experiments.

Thermo-Calc can be used to calculate some property data used for input into these codes, such as: density, volume fraction of phases, relative length change, coefficients of thermal expansion, heat capacity etc.

Thermo-Calc can also be used to "check" that phase transformations will not occur at recommended heat treat temperatures, particularly those that promote deleterious phases.

Density and lattice parameter

Lattice parameter of Ni-base alloy

△ Inconel 82 (Ni72-20Cr-3Mn-2.5Nb-1.0Fe-0.5...
□ Inconel 600 (Ni72-15.5Cr-8Fe-1.0Mn-0.5Cu-...
◇ Inconel 625 (Ni61-21.7Cr-3.9Fe-8.8Mo-3.9Nb...
⨯ Inconel 718 (Ni52.52-18.34Cr-5.10Nb-3.07M...
▽ Steel D9
+ Fe-20.5Cr-19.5Ni-19.4Mn-20.4Co, at%

Density of steels

△ Austenitic stainless steel
□ High alloy austenitic steel
◇ Ni-base alloy
⨯ High Cr and Ni
▽ Duplex
+ Ferritic stainless steel
∗ HSLA or carbon steel
⊙ Stainless steel alloyed by Al
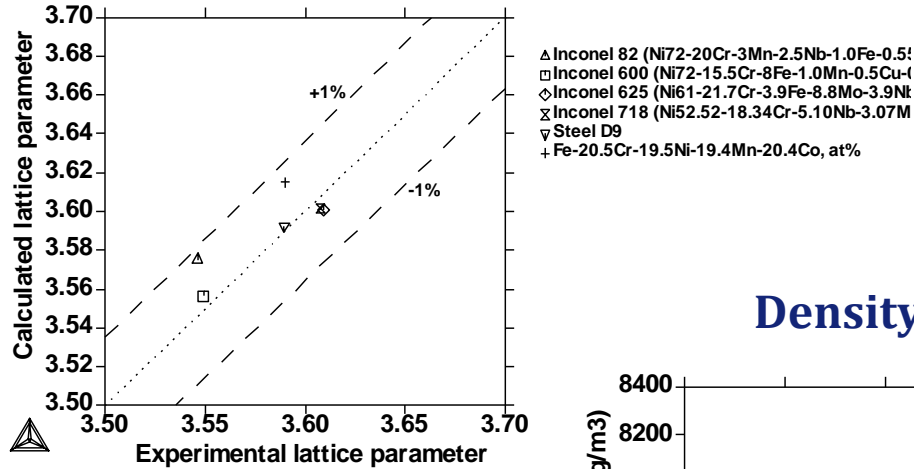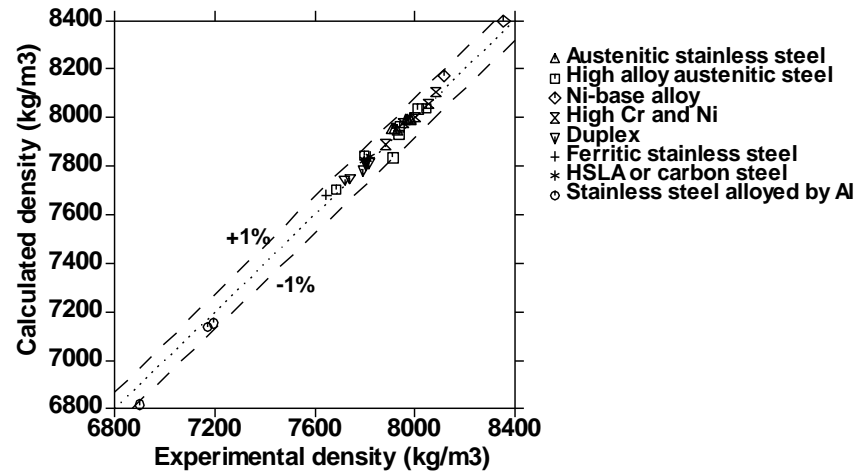
Density vs temperature

Steel 316: Fe-12Ni-17Cr-1.0Si-2.0Mn-2.5Mo-0.3Cu-0.08C (wt%)
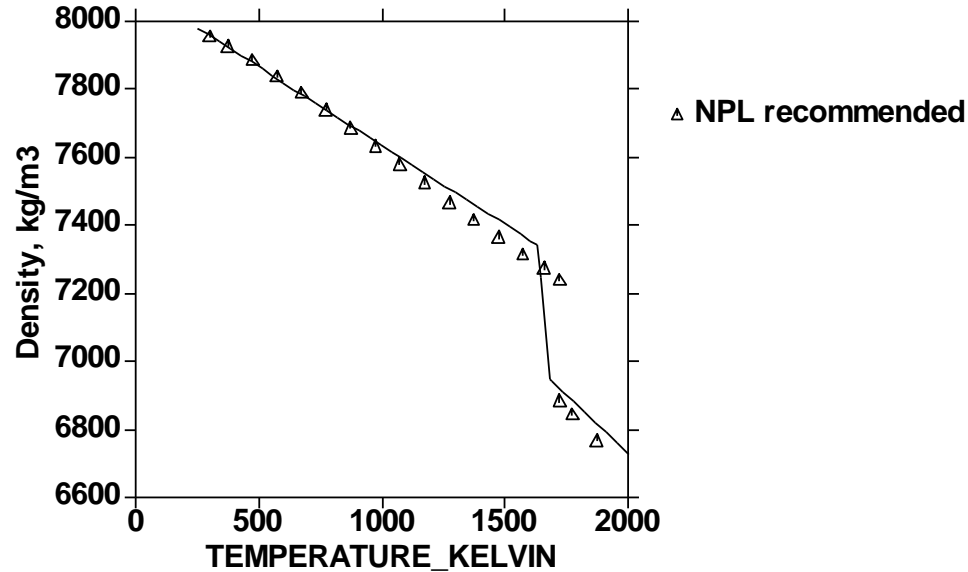
Combining with Scheil or DICTRA simulation, density variation during solidification can be calculated more properly.

Dilatometric curves

Fe-0.11% C-0.5%Mn-0.03%Si-0.01%Cr-0.02%Ni (in wt.%)
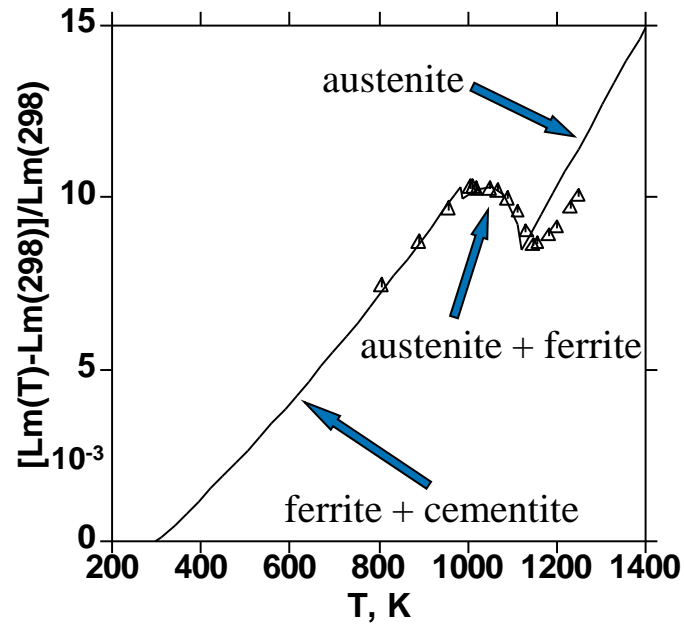
Materials challenges in additive manufacturing

- **Chemistry effects**
  - Segregation due to solidification
  - Laser can cause vaporization of certain elements
  - Surface area of powder can cause introduction of oxygen
  - Non-noble cover gasses can 'dissolve' into melt pool (eg. N)

- **Residual Stress**
  - Material properties (eg. Density) are not always known for metastable phases or novel compositions

- **Many alloys in use today were not designed for additive**
  - Many powders designed for HIP (no solidification) or welding (slower cooling rates)

- How can we better predict current material behavior, or design new materials that are resistant to these problems or even take advantage of some aspects of the additive process
  - i.e. use the reheating to form a strengthening precipitate
  - Tailor location specific properties by using wash passes when needed to increase strength in particular areas
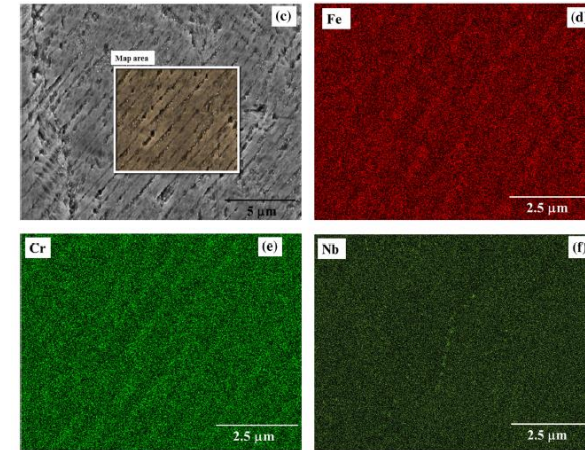
EDS Scans showing segregation of elements across dendrites in 17-4 PH Additive build

Cheruvathur et al "Additive Manufacturing of 17-4 PH Stainless Steel: Post-processing Heat Treatment to Achieve Uniform Reproducible Microstructure." JOM 68.3 (2016)

Stress relief Alloy 625 (I)

- Standard 'stress relief' treatment at 870°C causes copious precipitation of delta phase (deleterious), even after 30 minutes (atypical)

- Micrographs from Zhang et al. reveal that the delta phase starts to precipitate in the inter-dendritic regions, where DICTRA predicted higher Nb and Mo due to segregation

- Further heat treatment causes coarsening of the delta phase

- At first glance, it looks like this may be caused by solidification segregation – can we model this?
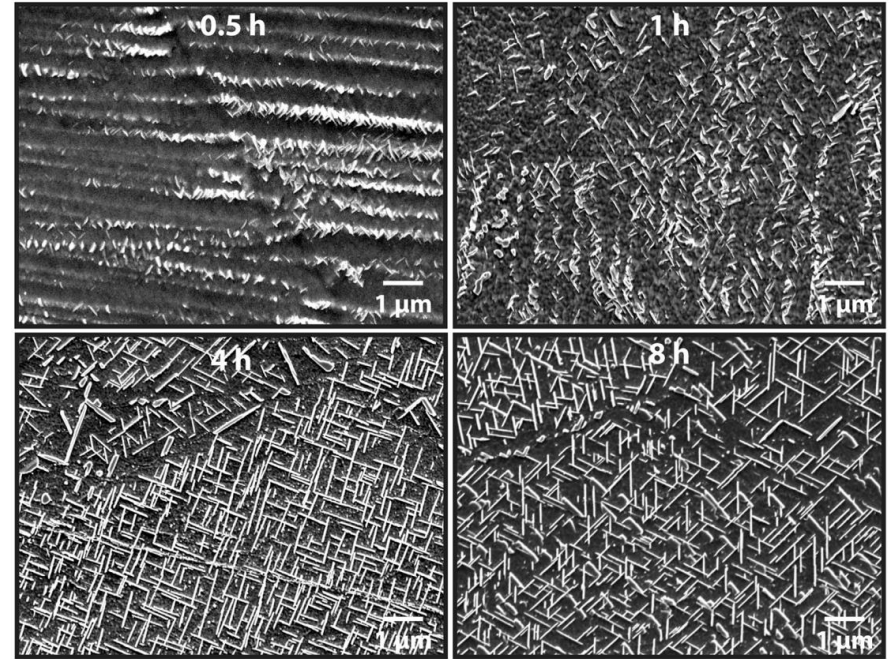
Zhang, Fan, et al. "Effect of heat treatment on the microstructural evolution of a nickel-based superalloy additive-manufactured by laser powder bed fusion." Acta Materialia (2018).

Stress relief Alloy 625 (II)

- Scheil predicts the most extreme segregation

- DICTRA can be used to simulate the back diffusion during cooling, as well as diffusion during reheat cycles

- Keller et al. simulated the segregation for 3 consecutive scan passes
    - Pass 2 re-melted the area of study (reset the segregation effectively) and is shown as the dashed line
    - Pass 3 caused reheating close to melting, and some diffusion to occur (solid line)
    - Authors found that subsequent passes were not of high enough temp/long enough time to cause significant diffusion
    - Reheating from subsequent passes is insufficient to homogenize the segregation
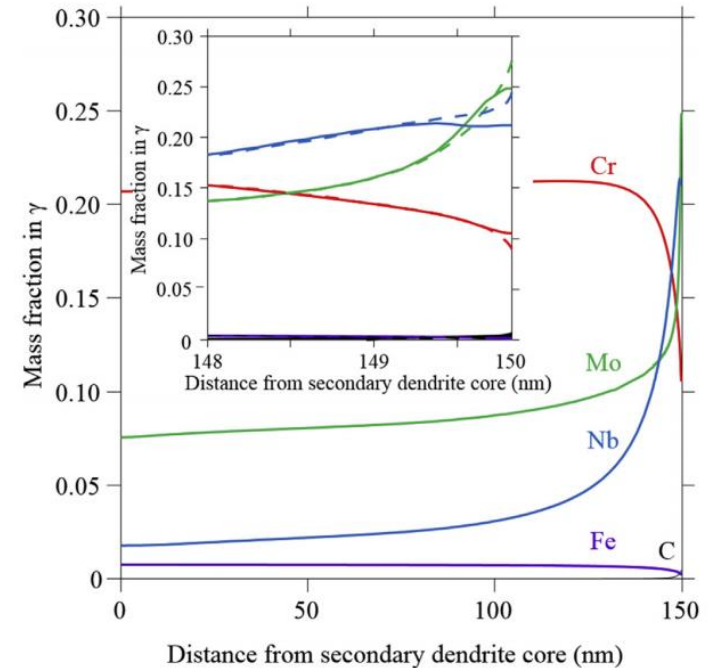
Keller, Trevor, et al. "Application of finite element, phase-field, and CALPHAD-based methods to additive manufacturing of Ni-based superalloys." *Acta materialia* 139 (2017): 244-253.

Stress relief Alloy 625 (III)

- Zhang et al. also performed TC-PRISMA simulations on two different representative compositions at 870°C
  - (a) from the dendrite core
  - (b) from the dendrite boundary/interdendritic region
- In both cases, gamma double prime forms first, then dissolves in favor of the delta phase (expected)
- The kinetics are sped up greatly for the segregated composition (increased Mo and Nb)
  - This lines up with what is seen in the 30 minute heat treatment
- Authors suggest performing a homogenization heat treatment above the delta solvus in a single phase region (determined with Thermo-Calc to be around 1150°C)
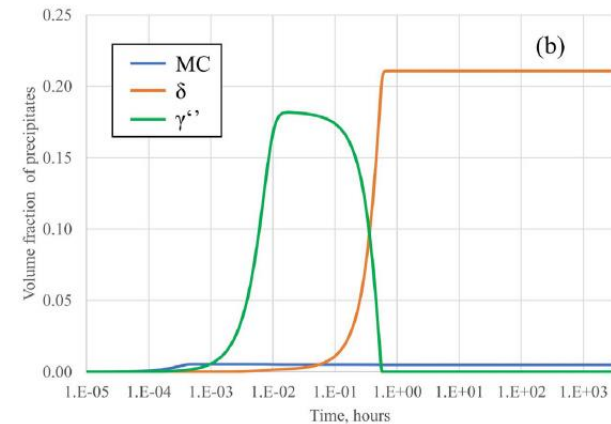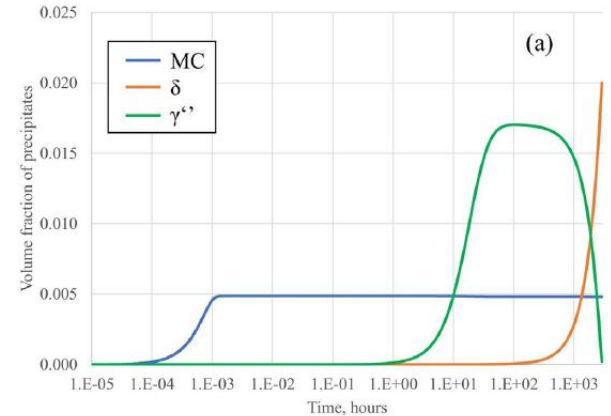
Quenching
(Martensite and Pearlite)

Carbon, low alloy and tool steels are quenched to produce controlled amounts of martensite in the microstructure.

Modeling Martensite transformations

- $\gamma \to \alpha$ diffusionless transformation by shear

- Martensite start temperature M_S is the temperature where the available driving force overcomes the barrier to switch the lattice to Martensite phase

Additional barrier for transformation to Martensite
→ how to model?
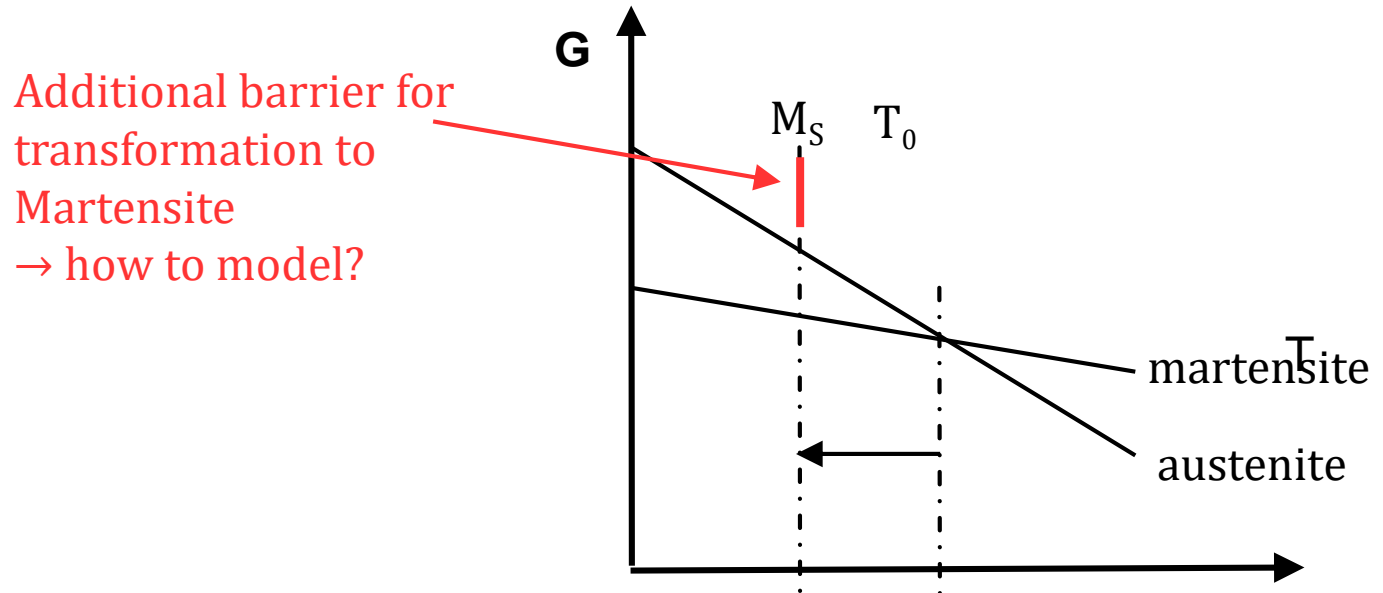
Semi-empirical model for describing the additional barrier (Stormvinter et al. Met. Mater Trans. 43A (2012)):

- takes into account the driving force to form martensite calculated by the CALPHAD method, with additional parameters added for various Fe-X binary systems

Modeling Martensite start temperatures (I)
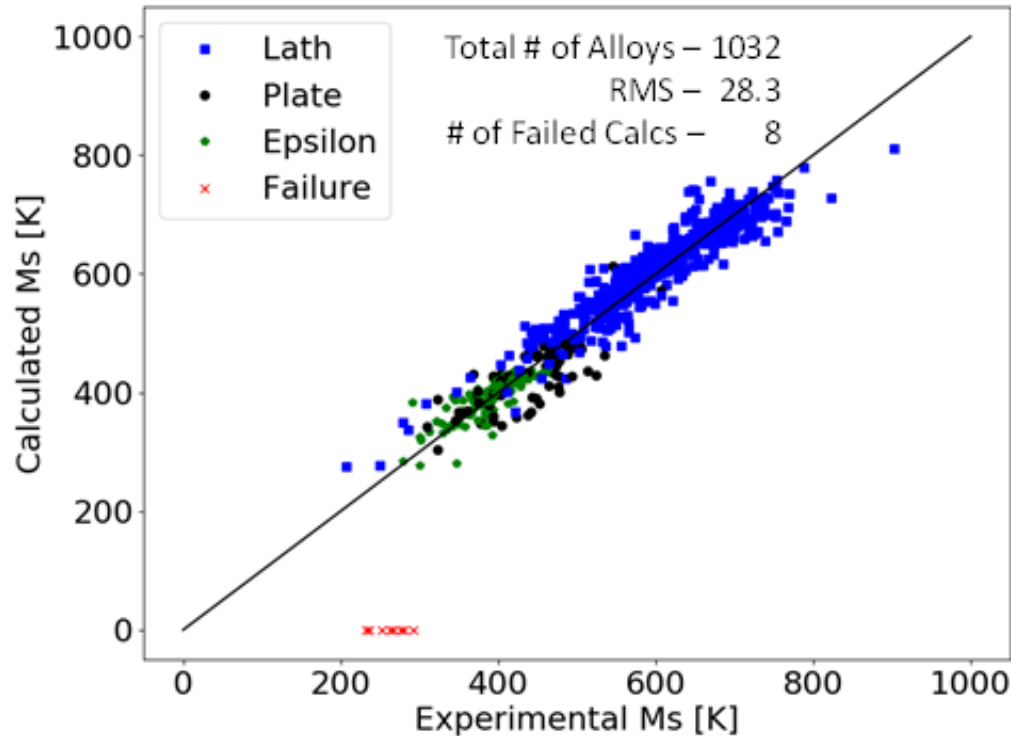
Comparison of calculated Ms against experimental Ms temperatures. Alloy compositions and Ms temperatures compiled from literature by Hanumantharaju.

Modeling Martensite start temperatures (II)

Fe	C	Mn	P	S	Si	Cr	Ni
Bal.	0.08-0.15	1	0.04	0.03	1	11.5-13.5	0.75

ASTM Composition spec (wt%) for 410 Martensitic Stainless Steel. Single values are a maximum

Calculated Ms temperature variation in 410 Stainless Steel composition specification
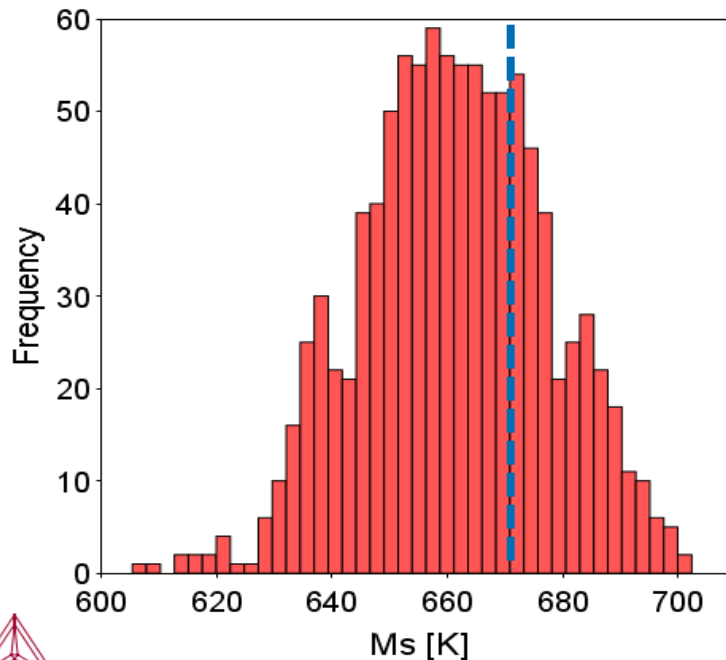
Measured value of 672K by Stone (OSU), 2017

Modeling Martensite fractions

- Based on model of Huyan et al. Met. Mat. Trans. A 2016

- Assumes first forming martensite morphology is only forming one.
- Austenite composition from eqm calc. at annealing temperature
- Grain size of austenite
- Austenite with smaller grain size is more stable

Pearlite is a common product of austenite decomposition in steels, typically alternating lamellae of ferrite and cementite

Most common form - spherical colonies consisting of alternating lamellae of ferrite and cementite.

We do not consider other less-common types of pearlite:
rod-shaped minority phase,
divorced or degenerate pearlite with discontinuous lamellae or rods, or non-spherical colony front of pearlite.

We do not consider the effects of stress, deformation, or preexisting phase(s) on pearlite formation

Steady-state model. Includes Fe, C, Mn, Cr, Mo, W, Si, Al, Ni, Co.

<u>Growth Rate:</u>
Growth rate v, lamellar spacing S, and phase constitution of pearlite are determined by a balance of driving force and dissipation.

<u>Driving force</u>
The total driving force for pearlite formation from austenite is the difference in Gibbs energy between the initial and final state

<u>Dissipation</u>
Total driving force is assumed to be dissipated by 4 processes:
(1) Formation of ferrite–cementite interface
(2) Pearlite–austenite interfacial friction
(3) Solute-drag force on pearlite–austenite interface
(4) Diffusion of elements, within austenite and along pearlite–austenite interface

Modeling pearlite (III)

Steel	C	Mn	P	S	Si	Co	Ni
3Ni	0.73	0.46	0.015	0.037	.554	0.01	2.91
1Co	0.95	0.48	0.038	0.024	0.25	0.95	0.01
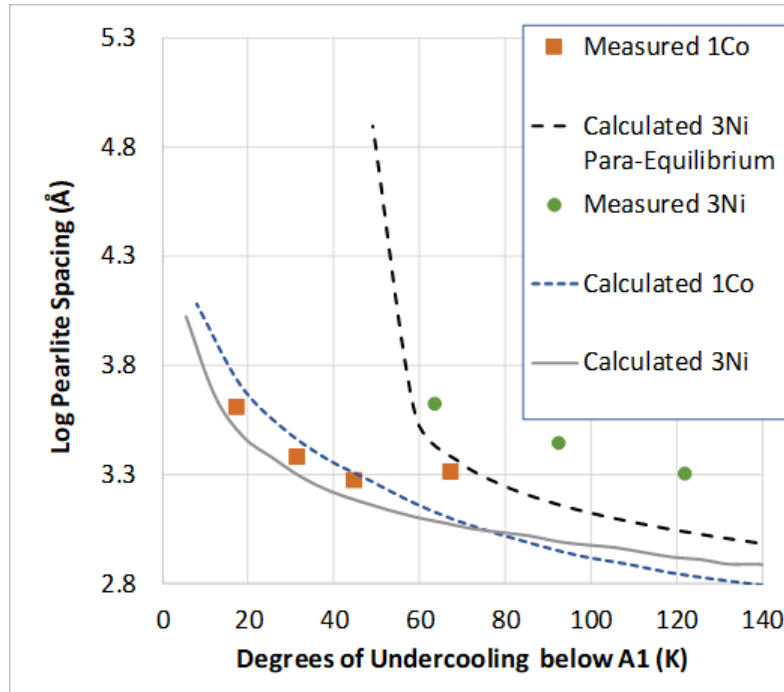
Pearlite spacing vs degree of undercooling below A1 temperature for two steels – 1Co and 3Ni. Experimental data from Pellissier et al.

Initially, the model for the 3Ni steel predicted much finer pearlite spacing than the experimental data.

In a review of the literature on pearlite growth, Ridley notes that steels with high Ni undergo a para-equilibrium decomposition to pearlite.

When the model was switched to account for the non-partitioning of substitutional elements (para-pearlite), the predicted pearlite spacing increased and the calculation is closer to the experimental data points

Variation of A1 temperature with composition
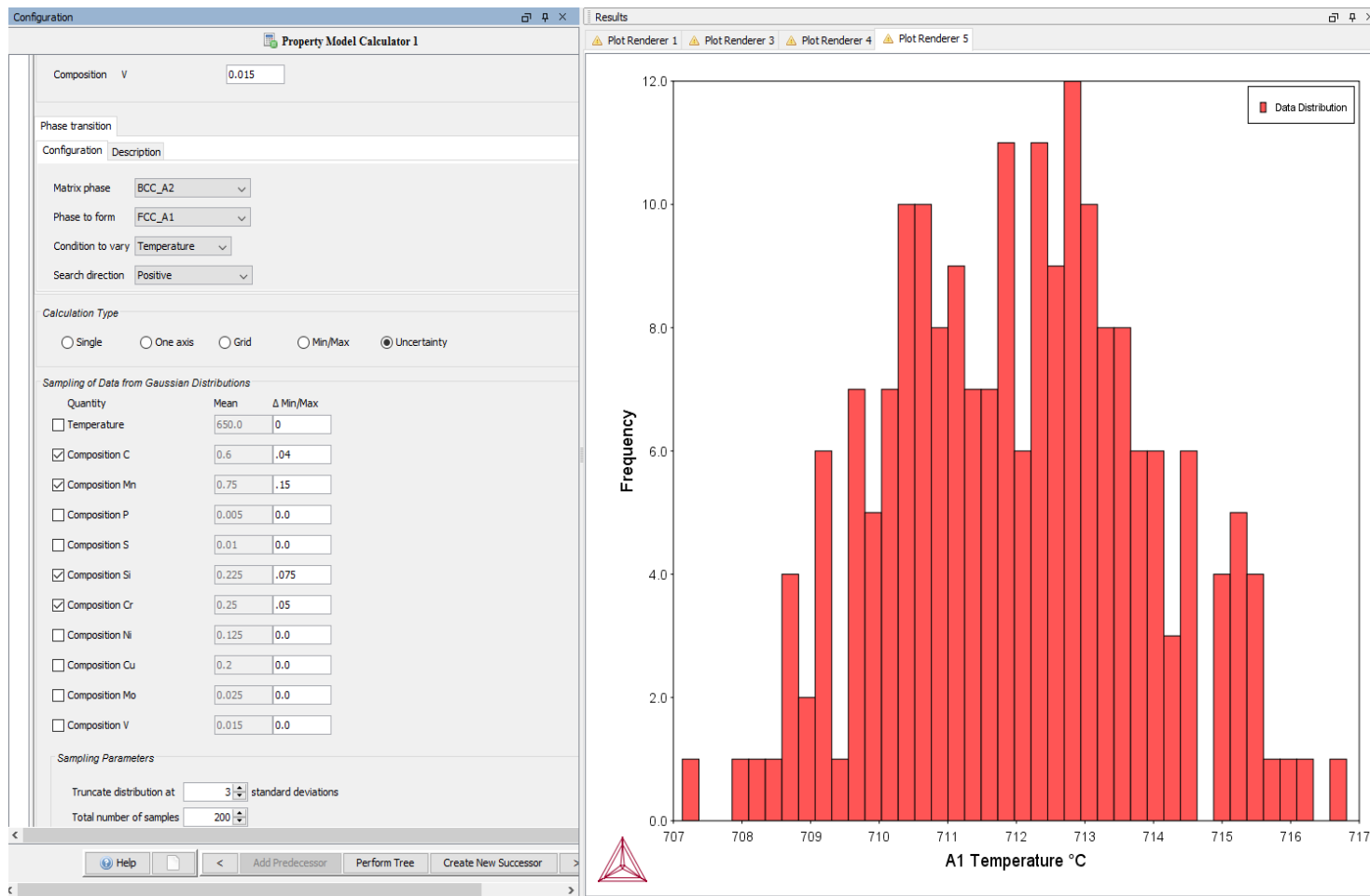
Summary

Materials are complex hierarchic systems and their microstructure determines the resulting properties and eventually performance

The microstructure is strongly dependent on processing conditions and composition. Capturing the knowledge and data needed for new processes and new materials can be time consuming, expensive and even prohibitive due to the time experiments may need to be run, etc.

To make good decisions, predict optimal processing windows, etc. requires understanding:

- the influence of composition and processing on structure
- the link between structure and resulting properties

CALPHAD provides a robust framework that integrates experimental and theoretical data and extends to multicomponent systems and allows predictions to be made for different heat treatment processes for both existing grades and new alloys.

Questions?